Nonlinear Fermi liquid transport through a quantum dot in asymmetric tunnel junctions

Kazuhiko Tsutsumi, Yoshimichi Teratani, Rui Sakano, and Akira Oguri

Phys. Rev. B **104**, 235147 — Published 23 December 2021

DOI: 10.1103/PhysRevB.104.235147

Nonlinear Fermi-liquid transport through a quantum dot in asymmetric tunnel junctions

Kazuhiko Tsutsumi,[1] Yoshimichi Teratani,[1,2] Rui Sakano,[3] and Akira Oguri[1,2]

[1] *Department of Physics, Osaka City University, Sumiyoshi-ku, Osaka 558-8585, Japan*
[2] *Nambu Yoichiro Institute of Theoretical and Experimental Physics, Sumiyoshi-ku, Osaka 558-8585, Japan*
[3] *Institute for Solid State Physics, the University of Tokyo, 5-1-5 Kashiwanoha, Kashiwa, Chiba 277-8581, Japan*

(Dated: December 6, 2021)

We study the nonlinear conductance through a quantum dot, specifically its dependence on the asymmetries in the tunnel couplings and bias voltages V, at low energies. Extending the microscopic Fermi-liquid theory for the Anderson impurity model, we obtain an exact formula for the steady current I up to terms of order V^3 in the presence of these asymmetries. The coefficients for the nonlinear terms are described in terms of a set of the Fermi-liquid parameters: the phase shift, static susceptibilities, and three-body correlation functions of electrons in the quantum dots, defined with respect to the equilibrium ground state. We calculate these correlation functions, using the numerical renormalization group approach (NRG), over a wide range of impurity-electron filling that can be controlled by a gate voltage in real systems. The NRG results show that the order V^2 nonlinear current is enhanced significantly in the valence fluctuation regime. It is caused by the order V energy shift of the impurity level, induced in the presence of the tunneling or bias asymmetry. Furthermore, in the valence fluctuation regime, we also find that the order V^3 nonlinear current exhibits a shoulder structure, for which the three-body correlations that evolve for large asymmetries play an essential role.

I. INTRODUCTION

The Kondo effect is one of the most interesting phenomena occurring in strongly correlated fermion systems [1, 2] and has been explored originally for dilute magnetic alloys [3–9]. It occurs also in quantum dots coupled to electron reservoirs [10–13], and has intensively been studied for three decades [14–17]. One of the advantages of the quantum dots for studying the Kondo effect is that the information of the many-body quantum states can be probed in a highly tunable way. For instance, recently development makes it possible to observe directly the Kondo screening cloud [18]. Furthermore, quantum dots have various variations, such as a single dot [19–30], multiple dots [31, 32], and the carbon-nanotube (CNT) dots [33–37]. The orbital degrees of freedom of the CNT dots also provides an interesting variety in the Kondo singlet state with the SU(4) symmetry [38–51].

Here we focus on the effects of the asymmetries in the tunnel junctions, which real quantum dots inevitably have more or less, on the nonlinear current I in the low-energy Fermi-liquid regime [4–9]. Specifically, we examine the asymmetry in the chemical potentials μ_L and μ_R of the source and drain electrodes, applied such that $eV \equiv \mu_L - \mu_R$, as well as the asymmetry in the tunnel couplings Γ_L and Γ_R.

These asymmetries vary the occupation number of quantum dots, and deform the Kondo cloud of conduction electrons which screens the local moment at temperatures $T \ll T^*$, lower than the Kondo energy scale T^*. The tunnel-coupling and bias asymmetries also affect the differential conductance dI/dV, which takes the following form at $T = 0$ up to terms of order $(eV)^2$,

$$\frac{dI}{dV} = g_0 \left[\sin^2\delta + C_V^{(2)} \frac{eV}{T^*} - C_V^{(3)} \left(\frac{eV}{T^*} \right)^2 + \cdots \right].$$

Here, $g_0 = (2e^2/h)\, 4\Gamma_L\Gamma_R/(\Gamma_L+\Gamma_R)^2$. The first term in the right-hand side with $\sin^2\delta$ represents the linear conductance, with δ the phase shift which is related to the average number of electrons in quantum dots. The nonlinear terms $C_V^{(2)}$ and $C_V^{(3)}$ include additional information about two-body and three-body correlations of electrons passing through the quantum dots, and it is the main topic of this work. These two terms depend strongly on the tunneling and bias asymmetries, especially $C_V^{(2)}$ emerges only in the presence of these asymmetries.

Effects of these asymmetries on the nonlinear currents in the Fermi-liquid regime have been developed for over a decade. Sela and Malecki [52] have derived $C_V^{(3)}$ for the particle-hole symmetric Anderson impurity model, for which the phase shift takes the value $\delta = \pi/2$ and $C_V^{(2)}$ identically vanishes even in the presence of the junction asymmetries. They have also shown using an effective Hamiltonian that $C_V^{(3)}$ for this case becomes independent of the junction-asymmetry parameters, $\Gamma_L - \Gamma_R$ and $(\mu_L+\mu_R)/2 - E_F$, in the limit of strong Coulomb interaction $U \to \infty$. Here, E_F is the Fermi level at equilibrium $eV = 0$. Aligia [53] has derived a more generalized formula which is applicable to arbitrary electron fillings, using the renormalized perturbation theory [54]. The formula for $C_V^{(2)}$ has successfully been derived in terms of the renormalized parameters of the Fermi-liquid and the junction-asymmetry parameters. However, the formula for $C_V^{(3)}$ away from half-filling was described in terms

of the second derivative of the real part of self-energy $\Sigma^r_\sigma(\omega)$ with respect to the frequencies ω whose behavior has been less understood until very recently. The lack of the knowledge about the second derivative of $\mathrm{Re}\,\Sigma^r_\sigma(\omega)$, which determines the higher-order energy shift of quasiparticles, makes the application range of their formula narrow.

Mora *et al* [47] have made an important step towards a deeper understanding of the higher-order contributions away from half-filling by extending Noziéres' phenomenological Fermi-liquid theory. They have derived the formulas for $C_V^{(2)}$ and $C_V^{(3)}$ for the SU(N) Kondo model, for which the number of impurity electrons m takes only integer values $m = 1, 2, \ldots, N-1$, taking also into account the tunnel asymmetry. More recently, Mora, Filippone *et al* [55, 56] have extended the Noziéres' description further to treat the Anderson impurity model for arbitrary electron fillings. The corresponding microscopic approach of Yamada-Yosida [6–9] has recently been expanded in the Keldysh formalism to explore higher-order Fermi-liquid corrections [57–59]. In particular, it has been clarified that the second derivative of $\mathrm{Re}\,\Sigma^r_\sigma(\omega)$ is determined by the three-body correlation functions of the impurity electrons, defined with respect to the equilibrium ground state. However, despite of these recent progress, effects of junction-asymmetries on the nonlinear transport still have not been explored in detail, so far, for quantum dots at arbitrary electron fillings [55–57, 59].

The purpose of this paper is to study how these asymmetries of the tunnel couplings and the bias voltages affect the nonlinear transport of correlated electrons away from half-filing. To this end, we derive the exact formulas for the coefficients $C_V^{(2)}$ and $C_V^{(3)}$ applicable to the asymmetric tunnel couplings and bias voltages. These coefficients are expressed in terms of the Fermi-liquid (FL) parameters defined with respect to the equilibrium ground state, i.e. the phase shift δ, the linear susceptibilities $\chi_{\sigma\sigma'}$ and the nonlinear susceptibilities $\chi^{[3]}_{\sigma_1\sigma_2\sigma_3}$. While $C_V^{(2)}$ is determined by δ and $\chi_{\sigma\sigma'}$, the coefficient $C_V^{(3)}$ depends also on the three-body correlations $\chi^{[3]}_{\sigma_1\sigma_2\sigma_3}$. Furthermore, we calculate $C_V^{(2)}$ and $C_V^{(3)}$ over a wide range of electron fillings, using the numerical renormalization group (NRG) [5, 60]. We have reported some preliminary results previously in a conference proceedings [61]. In the present paper, we describe further developments, including the complete formulation and explore behavior of $C_V^{(2)}$ and $C_V^{(3)}$ for various junction-asymmetries occurring in a wide parameter space.

The formula for $C_V^{(2)}$ agrees with the previous result of Aligia [53], and this term reflects the shift of impurity level induced at finite bias voltages eV in the presence of the tunnel-coupling and bias asymmetries. We find using also NRG that $C_V^{(2)}$ is enhanced significantly in the valence fluctuation regime.

The coefficient $C_V^{(3)}$ depends on two different three-body correlations $\chi^{[3]}_{\uparrow\uparrow\uparrow}$ and $\chi^{[3]}_{\uparrow\downarrow\downarrow}$ for the SU(2) Anderson impurity model away from half-filling. The three-body correlations are enhanced in the valence fluctuation regime, outside the Kondo ridge. We find that $C_V^{(3)}$ has a shoulder-type weak plateau in the gate-voltage dependence for large tunnel asymmetries. This structure is caused by the three-body correlations, especially by an enhancement of $\chi^{[3]}_{\uparrow\downarrow\downarrow}$ in the valence fluctuation regime. Recent experiment, which was carried out for highly symmetric tunnel junctions, have successfully demonstrated that the three-body contributions can be deduced from the nonlinear current [62]. Out results open the possibility to determine the contributions of $\chi^{[3]}_{\uparrow\uparrow\uparrow}$ and $\chi^{[3]}_{\uparrow\downarrow\downarrow}$ separately through measurements that can tune tunnel asymmetries.

This paper is organized as follows. In Sec. II, we describe the formulation and Fermi-liquid parameters. Section III is devoted to the derivation of the nonlinear transport coefficients through quantum dots. In Sec. IV, we describe the NRG results for quasiparticle parameters, including the three-body correlations. The NRG results for $C_V^{(2)}$ and $C_V^{(3)}$ are presented for junctions with tunnel and bias asymmetries in Secs. V and VI, respectively. Summary is given in Sec. VII.

II. FORMULATION

A. Anderson impurity model for quantum dots

We consider a single quantum dot coupled to two noninteracting leads, which is illustrated in Fig. 1 and is described by the Anderson impurity model [3]: $H = H_d + H_c + H_T$ with

$$H_d = \sum_{\sigma=\uparrow,\downarrow} \epsilon_{d\sigma} n_{d\sigma} + U\, n_{d\uparrow} n_{d\downarrow}\,, \tag{1}$$

$$H_c = \sum_{\nu=L,\,R} \sum_{\sigma=\uparrow,\downarrow} \int_{-D}^{D} d\epsilon\; \epsilon\, c^\dagger_{\epsilon\nu\sigma} c_{\epsilon\nu\sigma}\,, \tag{2}$$

$$H_T = \sum_{\nu=L,\,R} \sum_{\sigma=\uparrow,\downarrow} v_\nu \left(\psi^\dagger_{\nu,\,\sigma} d_\sigma + d^\dagger_\sigma\, \psi_{\nu,\,\sigma}\right), \tag{3}$$

$$\psi_{\nu,\,\sigma} \equiv \int_{-D}^{D} d\epsilon\, \sqrt{\rho_c}\, c_{\epsilon\nu\sigma}\,. \tag{4}$$

Here, $d^\dagger_\sigma$ creates an impurity electron with spin σ and energy $\epsilon_{d\sigma} \equiv \epsilon_d - \sigma b$. The parameter b represents a magnetic field, $n_{d\sigma} = d^\dagger_\sigma d_\sigma$, and U is the Coulomb interaction between electrons in the quantum dot. The operator $c^\dagger_{\epsilon\nu\sigma}$ creates a conduction electron with spin σ and continuous energy ϵ in the left (L) or right (R) lead. It satisfies the anticommutation relation $\left\{c_{\epsilon\nu\sigma}\,,\, c^\dagger_{\epsilon'\nu'\sigma'}\right\} = \delta(\epsilon - \epsilon')\,\delta_{\nu\nu'}\delta_{\sigma\sigma'}$ with $\delta(\epsilon - \epsilon')$ the Dirac δ function. We assume that the conduction band is flat over the range $-D < \epsilon < D$ with the constant density of states $\rho_c = 1/(2D)$. The linear combination of the conduction electrons $\psi_{\nu,\sigma}$ couples to the electrons in the quantum dot

via tunneling matrix element v_ν. The resonance width of the impurity level is given by $\Delta = \Gamma_L + \Gamma_R$ for $U = 0$, with $\Gamma_\nu = \pi\rho_c\nu^2$ the hybridization energy scale due to each of the leads ($\nu = L, R$).

B. Fermi-liquid parameters

We introduce here a set of the renormalized parameters which determine behavior of the transport coefficients, such as the conductance, current noise, and thermal conductivities, in the low-energy Fermi-liquid regime [51]. Properties of the quasiparticles can be described in terms of the retarded Green's function:

$$G^r_\sigma(\omega, T, eV) \equiv -i\int_0^\infty dt\, e^{i(\omega+i0^+)t}\left\langle \left\{ d_\sigma(t),\, d^\dagger_\sigma \right\} \right\rangle = \frac{1}{\omega - \epsilon_{d\sigma} + i\Delta - \Sigma^r_\sigma(\omega, T, eV)}\,, \tag{5}$$

$$A_\sigma(\omega, T, eV) = -\frac{1}{\pi}\,\mathrm{Im}\, G^r_\sigma(\omega,\, T,\, eV)\,. \tag{6}$$

Here, Σ^r_σ is the self-energy due to the Coulomb interaction and A_σ is the spectral function of impurity electrons. The nonequilibrium steady-state average $\langle\cdots\rangle$ is taken with the statistical density matrix, which is constructed at finite bias voltages eV and temperatures T, using the Keldysh formalism [63, 64].

The low-energy properties can be deduced specifically from the behavior of G^r_σ at small ω, T, and eV in the vicinity of the equilibrium ground state. In the following discussions, we use the notation,

$$\rho_{d\sigma}(\omega) \equiv A_\sigma(\omega, 0, 0), \qquad \Sigma^{\rm eq}_\sigma(\omega) \equiv \Sigma^r_\sigma(\omega, 0, 0). \tag{7}$$

For small frequencies ω, the Green's function takes the forms,

$$G^{\rm eq}_\sigma(\omega) \;\equiv\; G^r_\sigma(\omega, 0, 0) \simeq \frac{z_\sigma}{\omega - \widetilde{\epsilon}_{d\sigma} + i\widetilde{\Delta}_\sigma}\,. \tag{8}$$

Here, z_σ is the wavefunction renormalization factor, and $\widetilde{\Delta}_\sigma$ and $\widetilde{\epsilon}_{d\sigma}$ are the parameters that describe the renormalized resonance level, defined by

$$z_\sigma \;\equiv\; \left\{ 1 - \left.\frac{\partial\Sigma^{\rm eq}_\sigma(\omega)}{\partial\omega}\right|_{\omega=0} \right\}^{-1}, \tag{9}$$

$$\widetilde{\Delta}_\sigma \;\equiv\; z_\sigma\Delta, \qquad \widetilde{\epsilon}_{d\sigma} \;\equiv\; z_\sigma\Big[\,\epsilon_{d\sigma} + \Sigma^{\rm eq}_\sigma(0)\Big]\,. \tag{10}$$

The occupation number $\langle n_{d\sigma}\rangle$ of the impurity level determines ground-state properties. It can be obtained from the free energy $\Omega \equiv -T\log\left[\mathrm{Tr}\, e^{-H/T}\right]$ or the phase shift δ_σ using the Friedel sum rule,

$$\langle n_{d\sigma}\rangle \;=\; \frac{\partial\Omega}{\partial\epsilon_{d\sigma}} \xrightarrow{T\to 0} \frac{\delta_\sigma}{\pi}\,, \tag{11}$$

$$\delta_\sigma \;\equiv\; \cot^{-1}\left[\frac{\epsilon_{d\sigma} + \Sigma^{\rm eq}_\sigma(0)}{\Delta}\right]. \tag{12}$$

It also determines the density of states $\rho_{d\sigma}$, at the Fermi level $\omega = 0$, as

$$\rho_{d\sigma} = \frac{\sin^2\delta_\sigma}{\pi\Delta}\,. \tag{13}$$

Note that we are using the unit in which the Boltzmann constant is set as unity, i.e. $k_B = 1$.

The static linear susceptibilities $\chi_{\sigma\sigma'}$ are also essential parameters that determine the Fermi-liquid properties,

$$\chi_{\sigma\sigma'} \equiv -\frac{\partial^2\Omega}{\partial\epsilon_{d\sigma}\partial\epsilon_{d\sigma'}} = \int_0^{\frac{1}{T}} d\tau\, \langle T_\tau\, \delta n_{d\sigma}(\tau)\, \delta n_{d\sigma'}\rangle. \tag{14}$$

Here, $\delta n_{d\sigma} = n_{d\sigma} - \langle n_{d\sigma}\rangle$ is the fluctuation of the number of electrons in the dot from the average value, and T_τ is an imaginary-time ordering operator. The following Fermi-liquid relations hold at $T = 0$ between the susceptibilities and the parameters defined with respect to the self-energy [6, 8, 9],

$$\chi_{\sigma\sigma'} = \rho_{d\sigma}\widetilde{\chi}_{\sigma\sigma'}, \qquad \widetilde{\chi}_{\sigma\sigma'} \equiv \delta_{\sigma\sigma'} + \frac{\partial\Sigma^{\rm eq}_\sigma(0)}{\partial\epsilon_{d\sigma'}}, \tag{15}$$

and $1/z_\sigma = \widetilde{\chi}_{\sigma\sigma}$. From this relation, the T-linear specific heat of the impurity electrons $\mathcal{C}^{\rm heat}_{\rm imp}$ has been shown to be expressed in terms of the diagonal part of the linear susceptibility [6, 8, 9], as

$$\mathcal{C}^{\rm heat}_{\rm imp} \;=\; \frac{\pi^2}{3}\sum_\sigma \chi_{\sigma\sigma}\, T\,. \tag{16}$$

It has recently been shown that the static three-body correlation functions $\chi^{[3]}_{\sigma_1\sigma_2\sigma_3}$ also contribute to the next-leading terms of the transport coefficients when the system does not have particle-hole symmetry or time-reversal symmetry [55–59],

$$\chi^{[3]}_{\sigma_1\sigma_2\sigma_3} \;\equiv\; -\frac{\partial^3\Omega}{\partial\epsilon_{d\sigma_1}\partial\epsilon_{d\sigma_2}\partial\epsilon_{d\sigma_3}} = \frac{\partial\chi_{\sigma_1\sigma_2}}{\partial\epsilon_{d\sigma_3}} = -\int_0^{\frac{1}{T}} d\tau_1 \int_0^{\frac{1}{T}} d\tau_2\, \langle T_\tau \delta n_{d\sigma_1}(\tau_1)\, \delta n_{d\sigma_2}(\tau_2)\, \delta n_{d\sigma_3}\rangle\,. \tag{17}$$

This function has permutation symmetry for the indexes: $\chi^{[3]}_{\sigma_1\sigma_2\sigma_3} = \chi^{[3]}_{\sigma_2\sigma_1\sigma_3} = \chi^{[3]}_{\sigma_3\sigma_2\sigma_1} = \chi^{[3]}_{\sigma_1\sigma_3\sigma_2} = \cdots$.

The main subject of this paper is to clarify how the three-body correlations contribute to the nonlinear transport when the additional asymmetries are present in the tunnel couplings and bias voltages. We also focus on the impurity level shift which is induced by the bias voltages in the presence of these asymmetries and demonstrate how it affects order $(eV)^2$ nonlinear current using the NRG.

III. CURRENT FORMULA FOR JUNCTIONS WITH TUNNEL AND BIAS ASYMMETRIES

In this section, we derive the formula for the nonlinear current in the low-energy Fermi-liquid regime, taking

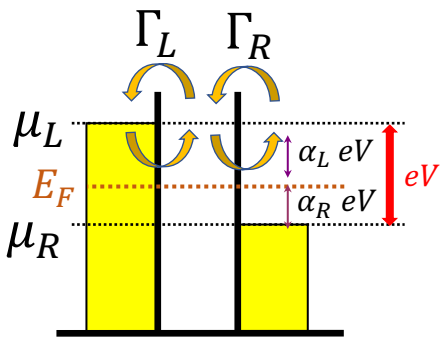

FIG. 1. Schematic diagram of a quantum dot coupled to two leads via the tunnel couplings Γ_L and Γ_R. The bias voltage $eV = \mu_L - \mu_R$ is applied in a way such that $\mu_L = E_F + \alpha_L eV$ and $\mu_R = E_F - \alpha_R eV$, with $\alpha_L + \alpha_R = 1$. The chemical potentials of the left and right leads are measured from the Fermi energy at equilibrium $E_F = 0$. The tunnel coupling is smaller for the barrier with thicker width.

into account the asymmetries in the tunnel couplings and applied bias voltages.

A. Steady-state average of nonlinear current

We start with a quantum dot embedded in a tunnel junction as illustrated in Fig. 1. The bias voltage $eV = \mu_L - \mu_R$ is applied through the chemical potential in the left lead $\mu_L = \alpha_L\, eV$ and that in the right lead $\mu_R = -\alpha_R\, eV$. Here, the parameters α_L and α_R are introduced such that $\alpha_L + \alpha_R = 1$ in order to specify the way how the system has been driven from equilibrium. For $\alpha_L = \alpha_R = 0.5$, it describes the bias is symmetric with respect to the Fermi level $E_F = 0$ at equilibrium. In an extreme $\alpha_L = 1$ and $\alpha_R = 0$, it describes the situation where the drain is grounded at $\mu_R = E_F = 0$ and the bias voltage is applied to the source side $\mu_L = eV$, corresponding to one natural experimental situation.

Specifically, in this work, we examine transport properties of the Anderson impurity for $N = 2$ at zero field $b = 0$, where $\epsilon_{d\sigma} \equiv \epsilon_d$. In this case, the system has an SU(2) rotational symmetry in the spin space, and thus the components of the correlation functions are related to each other, as $\chi_{\uparrow\uparrow} = \chi_{\downarrow\downarrow}$, $\chi^{[3]}_{\uparrow\uparrow\uparrow} = \chi^{[3]}_{\downarrow\downarrow\downarrow}$, and $\chi^{[3]}_{\uparrow\downarrow\downarrow} = \chi^{[3]}_{\uparrow\uparrow\downarrow}$. Since the two spin components, $\uparrow$ and $\downarrow$, become equivalent in this case, we also use a simplified notation suppressing the suffix for spin degrees of freedom from the phase shift δ, the impurity density of states ρ_d defined in Eq. (13), and the self-energy. Furthermore, the characteristic energy scale T^* and the Wilson ratio R can be expressed in the form,

$$T^* \equiv \frac{1}{4\chi_{\uparrow\uparrow}}, \qquad R \equiv 1 - \frac{\chi_{\uparrow\downarrow}}{\chi_{\uparrow\uparrow}}. \tag{18}$$

Non-equilibrium current through a quantum dot can be calculated using a Landauer-type formula [63, 64],

$$I = \frac{2e}{h}\frac{4\Gamma_L\Gamma_R}{(\Gamma_L+\Gamma_R)^2} \times \int_{-\infty}^{\infty} d\omega \Big[f(\omega-\mu_L) - f(\omega-\mu_R)\Big]\, \pi\Delta A(\omega,\, T,\, eV)\,. \tag{19}$$

Here, $f(\omega) = [e^{\beta\omega}+1]^{-1}$ is the Fermi distribution function, and $A(\omega,\, T,\, eV)$ is the spectral function defined by Eq. (6). Thus at low energies, behavior of the spectral function $A(\omega,\, T,\, eV)$ for small ω, T, and eV determines the current. In particular at zero temperature, the spectral weight in the bias window region $\mu_R \le \omega \le \mu_L$ contribute to the current I flowing through the quantum dot,

$$I \xrightarrow{T\to 0} \frac{2e}{h}\frac{4\Gamma_L\Gamma_R}{(\Gamma_L+\Gamma_R)^2}\int_{\mu_R}^{\mu_L} d\omega\, \pi\Delta A(\omega,\, 0,\, eV)\,. \tag{20}$$

In order to study the nonlinear current in the Fermi-liquid regime, we use the exact low-energy asymptotic form of the self-energy, obtained recently up to terms of order ω^2, T^2, and $(eV)^2$ [56, 59], specifically the extended one which is applicable to asymmetric junctions and bias voltages, [59]

$$\begin{aligned}\epsilon_d + \mathrm{Re}\,\Sigma^r(\omega,T,eV) = {}& \Delta\cot\delta \;+\; (1-\widetilde{\chi}_{\uparrow\uparrow})\,\omega \;+\; \frac{1}{2}\frac{\partial\widetilde{\chi}_{\uparrow\uparrow}}{\partial\epsilon_{d\uparrow}}\omega^2 \\ & + \frac{1}{6}\frac{1}{\rho_d}\frac{\partial\chi_{\uparrow\downarrow}}{\partial\epsilon_{d\downarrow}}\left[\frac{3\Gamma_L\Gamma_R}{(\Gamma_L+\Gamma_R)^2}(eV)^2 + (\pi T)^2\right] \\ & - \widetilde{\chi}_{\uparrow\downarrow}\alpha\, eV + \frac{\partial\widetilde{\chi}_{\uparrow\downarrow}}{\partial\epsilon_{d\uparrow}}\alpha\, eV\omega \;+\; \frac{1}{2}\frac{\partial\widetilde{\chi}_{\uparrow\downarrow}}{\partial\epsilon_{d\downarrow}}\alpha^2(eV)^2 + \cdots,\end{aligned} \tag{21}$$

$$\mathrm{Im}\,\Sigma^r(\omega,T,eV) = -\frac{\pi}{2}\frac{1}{\rho_d}\chi^2_{\uparrow\downarrow}\left[(\omega-\alpha eV)^2 + \frac{3\Gamma_L\Gamma_R}{(\Gamma_L+\Gamma_R)^2}(eV)^2 + (\pi T)^2\right] + \cdots. \tag{22}$$

The parameter α plays a central role throughout this work, and it consists of the following two parts which represent the tunnel and the bias asymmetries, respectively,

$$\alpha \equiv \frac{\alpha_L\Gamma_L - \alpha_R\Gamma_R}{\Gamma_L+\Gamma_R} = \frac{1}{2}(\alpha_L-\alpha_R) + \frac{1}{2}\frac{\Gamma_L-\Gamma_R}{\Gamma_L+\Gamma_R}. \tag{23}$$

Note that $\alpha_L + \alpha_R = 1$. The bias asymmetry can also be described by a single parameter, as $\alpha_L = (1+\alpha_{\rm dif})/2$ and $\alpha_R = (1-\alpha_{\rm dif})/2$, with

$$\alpha_{\rm dif} \equiv \alpha_L - \alpha_R\,, \tag{24}$$

which takes values in the range $-1 \le \alpha_{\rm dif} \le 1$. The coefficients for low-energy expansion of the self-energy up

TABLE I. Low-energy expansion of dI/dV for $N = 2$ at $T = 0$. The tunnel and bias asymmetries enter through the parameters $(\Gamma_L - \Gamma_R)/\Delta$ and $\alpha_{\rm dif} \equiv \alpha_L - \alpha_R$, respectively, in addition to the factor $4\Gamma_L\Gamma_R/(\Gamma_L + \Gamma_R)^2$ in front. The characteristic energy scale $T^* = 1/(4\chi_{\uparrow\uparrow})$ and the Wilson ratio $R - 1 = -\chi_{\uparrow\downarrow}/\chi_{\uparrow\uparrow}$ are determined by the linear susceptibilities $\chi_{\uparrow\uparrow}$ and $\chi_{\uparrow\downarrow}$. The three-body contributions $\chi^{[3]}_{\uparrow\uparrow\uparrow}$ and $\chi^{[3]}_{\uparrow\downarrow\downarrow}$ enter through dimensionless parameters $\Theta_{\rm I}$ and $\Theta_{\rm II}$.

$\frac{dI}{dV} = \frac{2e^2}{h}\frac{4\Gamma_L\Gamma_R}{(\Gamma_L+\Gamma_R)^2}\left[\sin^2\delta + C_V^{(2)}\left(\frac{eV}{T^*}\right) - C_V^{(3)}\left(\frac{eV}{T^*}\right)^2 + \cdots\right], \quad \Theta_{\rm I} \equiv \frac{\sin 2\delta}{2\pi\chi_{\uparrow\uparrow}^2}\chi^{[3]}_{\uparrow\uparrow\uparrow}, \quad \Theta_{\rm II} \equiv \frac{\sin 2\delta}{2\pi\chi_{\uparrow\uparrow}^2}\chi^{[3]}_{\uparrow\downarrow\downarrow},$
$C_V^{(3)} = \frac{\pi^2}{64}(W_V + \Theta_V), \qquad C_V^{(2)} = \frac{\pi}{4}\left[\alpha_{\rm dif} - \left(\alpha_{\rm dif} + \frac{\Gamma_L-\Gamma_R}{\Gamma_L+\Gamma_R}\right)(R-1)\right]\sin 2\delta,$
$W_V = -\cos 2\delta\left[1 + 3\alpha_{\rm dif}^2 - 6\alpha_{\rm dif}\left\{\alpha_{\rm dif} + \frac{\Gamma_L-\Gamma_R}{\Gamma_L+\Gamma_R}\right\}(R-1) + \left\{5 + 3\alpha_{\rm dif}^2 + 6\,\alpha_{\rm dif}\frac{\Gamma_L-\Gamma_R}{\Gamma_L+\Gamma_R}\right\}(R-1)^2\right],$
$\Theta_V = \left[1 + 3\alpha_{\rm dif}^2\right]\Theta_{\rm I} + 3\left[1 + 3\alpha_{\rm dif}^2 + 4\alpha_{\rm dif}\frac{\Gamma_L-\Gamma_R}{\Gamma_L+\Gamma_R}\right]\Theta_{\rm II}.$

to quadratic order terms, given in Eqs. (21) and (22), are described by five Fermi-liquid parameters, i.e. the phase shift δ, the susceptibilities $\chi_{\uparrow\uparrow}$ and $\chi_{\uparrow\downarrow}$, and the two three-body correlations $\chi^{[3]}_{\uparrow\uparrow\uparrow}$ and $\chi^{[3]}_{\uparrow\downarrow\downarrow}$. In particular, the three-body correlations determine the quadratic-order terms of the real part $\mathrm{Re}\,\Sigma^r(\omega, T, eV)$.

B. Current formula for the local Fermi liquid

We obtain the generic expression for the differential conductance dI/dV which is exact up to terms of order T^2 and $(eV)^2$, substituting the above asymptotic form of the self-energy into the energy denominator of the Green's function given in Eq. (5), and then carrying out the ω integral in the Meir-Wingreen formula [see Appendix A],

$$\frac{dI}{dV} = \frac{2e^2}{h}\frac{4\Gamma_L\Gamma_R}{(\Gamma_L+\Gamma_R)^2}\left[\sin^2\delta - C_T\left(\frac{\pi T}{T^*}\right)^2 + C_V^{(2)}\left(\frac{eV}{T^*}\right) - C_V^{(3)}\left(\frac{eV}{T^*}\right)^2 + \cdots\right]. \quad (25)$$

The first two terms in the right-hand side correspond to the linear conductance: the coefficient C_T for the T^2 term is given by

$$C_T = \frac{\pi^2}{48}\left(W_T + \Theta_{\rm I} + \Theta_{\rm II}\right), \quad (26)$$
$$W_T = -\cos 2\delta\left[1 + 2(R-1)^2\right],$$

with $\Theta_{\rm I}$ and $\Theta_{\rm II}$ the dimensionless three-body correlation functions, defined by

$$\Theta_{\rm I} \equiv \frac{\sin 2\delta}{2\pi\chi_{\uparrow\uparrow}^2}\chi^{[3]}_{\uparrow\uparrow\uparrow}, \qquad \Theta_{\rm II} \equiv \frac{\sin 2\delta}{2\pi\chi_{\uparrow\uparrow}^2}\chi^{[3]}_{\uparrow\downarrow\downarrow}. \quad (27)$$

Note that $\sin 2\delta$ is proportional to the derivative of the spectral weight, as

$$\sin 2\delta = \frac{\Delta}{\chi_{\uparrow\uparrow}}\left.\frac{\partial\rho_d(\omega)}{\partial\omega}\right|_{\omega=0}. \quad (28)$$

The linear-response part of the differential conductance depends on the tunnel asymmetry only through the prefactor $4\Gamma_L\Gamma_R/(\Gamma_L+\Gamma_R)^2$ in the right-hand side of Eq. (25), and it dose not depend on the bias asymmetry $\alpha_{\rm dif}$.

In contrast, the nonlinear part of dI/dV, i.e. $C_V^{(2)}$ and $C_V^{(3)}$, depend essentially on the tunnel and bias asymmetries:

$$C_V^{(2)} = \frac{\pi}{4}\left[\alpha_{\rm dif} - \left(\alpha_{\rm dif} + \frac{\Gamma_L-\Gamma_R}{\Gamma_L+\Gamma_R}\right)(R-1)\right]\sin 2\delta, \quad (29)$$

$$C_V^{(3)} = \frac{\pi^2}{64}\left(W_V + \Theta_V\right). \quad (30)$$

Here, W_V and Θ_V represent the two-body and three-body contributions,

$$W_V = -\cos 2\delta\left[1 + 3\alpha_{\rm dif}^2 - 6\alpha_{\rm dif}\left(\alpha_{\rm dif} + \frac{\Gamma_L-\Gamma_R}{\Gamma_L+\Gamma_R}\right)(R-1) + \left(5 + 3\alpha_{\rm dif}^2 + 6\,\alpha_{\rm dif}\frac{\Gamma_L-\Gamma_R}{\Gamma_L+\Gamma_R}\right)(R-1)^2\right], \quad (31)$$

$$\Theta_V = \left[1 + 3\alpha_{\rm dif}^2\right]\Theta_{\rm I} + 3\left[1 + 3\alpha_{\rm dif}^2 + 4\alpha_{\rm dif}\frac{\Gamma_L-\Gamma_R}{\Gamma_L+\Gamma_R}\right]\Theta_{\rm II}. \quad (32)$$

In order to express the coefficients in this form, we have used Eqs. (23), (24) and the following relation between the asymmetry parameters due to $\alpha_L + \alpha_R = 1$,

$$\alpha^2 + \frac{\Gamma_L\Gamma_R}{\Delta^2} = \frac{1}{4}\left[1 + \alpha_{\rm dif}^2 + 2\alpha_{\rm dif}\frac{\Gamma_L-\Gamma_R}{\Gamma_L+\Gamma_R}\right]. \quad (33)$$

Note that the dependence of $C_V^{(2)}$ and $C_V^{(3)}$ on tunnel asymmetries $(\Gamma_L-\Gamma_R)/\Delta$ enters through the self-energy given in Eqs. (21) and (22), and thus it emerges only for interacting-electron systems with finite U. While $C_V^{(2)}$ depends on the Coulomb interaction only through the real part of the self-energy, the coefficient $C_V^{(3)}$ depends also on the ω^2 and $(eV)^2$ imaginary parts that destroy phase coherence [67, 68]. In contrast, the bias asymmetry $\alpha_{\rm dif}$ affects these coefficients already at $U=0$.

The expression of $C_V^{(2)}$ given in Eq. (29) agrees with the previous result derived by Aligia using the renormalized perturbation theory [53]. For the current of order $(eV)^3$, the coefficients Θ_V and W_V represent the three-body contributions and the two-body ones, respectively. Our result for $C_V^{(3)}$ extends the previous one which was derived for the particle-hole symmetric case by Sela and Malecki [52] to the particle-hole asymmetric case taking place away from half-filling. These formulas for dI/dV in the Fermi-liquid regime is also summarized in the Table I for quick reference.

1. *Inversion of (α_L,Γ_L) and (α_R,Γ_R)*

One of the common features of the Landauer type conductance, defined in Eq. (19), is a factor $4\Gamma_L\Gamma_R/(\Gamma_L+\Gamma_R)^2$ in front that suppresses the current for asymmetric tunnel junctions. The explicit expressions of dI/dV given in the above show explicitly that the nonlinear current components of current depend further on the junction asymmetries. The coefficients $C_V^{(2)}$ and $C_V^{(3)}$ vary as the tunnel and bias asymmetries enter also through the terms with the parameters $(\Gamma_L-\Gamma_R)/\Delta$ and $\alpha_{\rm dif}$ in Eqs. (29)–(32). Thus, these coefficients can be regarded as functions of the two asymmetry parameters $\alpha_{\rm dif}$ and Γ_L/Γ_R for a fixed value of $\Delta=\Gamma_L+\Gamma_R$.

The order $(eV)^2$ component has the following properties with respect to an inversion of (α_L,Γ_L) and (α_R,Γ_R),

$$C_V^{(2)}(\alpha_{\rm dif},\Gamma_L/\Gamma_R) \,=\, -\,C_V^{(2)}(-\alpha_{\rm dif},\Gamma_R/\Gamma_L)\,. \qquad (34)$$

It shows that the order $(eV)^2$ nonlinear current emerges when the system has the tunnel or the bias asymmetry, i.e. $\alpha_{\rm dif}\neq 0$ or $\Gamma_L\neq\Gamma_R$. In addition, Eq. (29) also shows that this component of I vanishes at half-filling, where $\delta=\pi/2$.

Similarly, the order $(eV)^3$ component is invariant with respect to the same inversion of $L\Leftrightarrow R$,

$$C_V^{(3)}(\alpha_{\rm dif},\Gamma_L/\Gamma_R) \,=\, C_V^{(3)}(-\alpha_{\rm dif},\Gamma_R/\Gamma_L)\,. \qquad (35)$$

In the rest of this paper, we demonstrate how the coefficients $C_V^{(2)}$ and $C_V^{(3)}$ vary over a wide range of the asymmetries and of the gate voltage, by which the ground state evolves from the Kondo regime towards the valence fluctuation regime.

IV. NRG RESULTS FOR FERMI-LIQUID PARAMETERS

We discuss in this section how the five Fermi-liquid (FL) parameters, δ, $\chi_{\uparrow\uparrow}$, $\chi_{\uparrow\downarrow}$, $\chi^{[3]}_{\uparrow\uparrow\uparrow}$, and $\chi^{[3]}_{\uparrow\downarrow\downarrow}$, evolve as the impurity level ϵ_d and the Coulomb interaction U are varied [5, 65]. These parameters are defined with respect to the equilibrium ground state, for which only a single *bonding*-type channel constructed by a linear-combination of the left and right conduction bands, $\psi^{\rm bond}_\sigma \equiv (v_L\,\psi_{L,\sigma}+v_R\,\psi_{R,\sigma})/\sqrt{v_L^2+v_R^2}$, is coupled to the impurity level and the other channel is separated. Thus, the FL parameters themselves do not depend on the tunnel nor bias asymmetries, and numerical results have been reported previously [55–59]. Nevertheless, behaviors of the FL parameter determine the coefficients of the nonlinear current $C_V^{(2)}$ and $C_V^{(3)}$, defined in Eqs. (29)–(32), with the other parameters $(\Gamma_L-\Gamma_R)/\Delta$ and $\alpha_{\rm dif}$, and play an essential role also for transport through junctions with the tunnel and bias asymmetries.

We have calculated the FL parameters with the NRG approach, choosing the discretization parameter to be $\Lambda=2.0$ and keeping $N_{\rm trunc}=3600$ low-lying energy states at each step of the iterative procedure. Our NRG code uses the global $\mathrm{U}(1)\otimes\mathrm{SU}(2)$ symmetries and the method described in Ref. 37 and 65. The three-body correlation functions have been deduced from the linear susceptibilities $\chi_{\uparrow\uparrow}$ and $\chi_{\uparrow\downarrow}$, using the following relations,

$$\chi^{[3]}_{\uparrow\uparrow\uparrow}=\frac{\partial\chi_{\uparrow\uparrow}}{\partial\epsilon_d}-\frac{1}{2}\,\frac{\partial\chi_{\uparrow\downarrow}}{\partial\epsilon_d}, \qquad \chi_{\uparrow\downarrow\downarrow}=\frac{1}{2}\,\frac{\partial\chi_{\uparrow\downarrow}}{\partial\epsilon_d}\,. \qquad (36)$$

Figure 2 shows the FL parameters $\langle n_{d\sigma}\rangle$, $\sin^2\delta$, the Wilson ratio $R-1$, and the inverse of T^* as functions of ϵ_d/U, obtained with the NRG for several different values of the Coulomb interaction $U/(\pi\Delta)$ taking $\pi\Delta=D/100$ [59]. Note that the system has particle-hole (PH) symmetry at $\epsilon_d=-U/2$.

We can see in the top panel (a) that the average number of impurity electrons, $\langle n_{d\sigma}\rangle=\delta/\pi$, shows the Coulomb staircase behavior, and the impurity level is singly occupied $\langle n_{d\uparrow}+n_{d\downarrow}\rangle\simeq 1.0$ in the Kondo regime $-U\lesssim\epsilon_d\lesssim 0$. The second panel, Fig. 2(b), shows $\sin^2\delta$, which corresponds to the zero-bias conductance. Thus, the broad peak of the unitary-limit value $\sin^2\delta\simeq 1.0$ at $-U\lesssim\epsilon_d\lesssim 0$ describes the Kondo ridge of the conductance at $T=0$. The Wilson ratio, plotted in Fig. 2(c), also shows a broad ridge the height of which reaches the strong-coupling value $R-1\simeq 1$ for $U\gtrsim 3.0\pi\Delta$ in the Kondo regime. The bottom panel (d) shows the ϵ_d dependence of $1/T^*$, which is normalized by T_K defined as the value of T^* at half-filing $\epsilon_d=-U/2$. The characteristic temperature T^* increases rapidly away from half-filling as ϵ_d deviates from the particle-hole symmetric point.

These results also demonstrate clearly that the Fermi-liquid parameters approach the noninteracting values far away from half-filling $|\epsilon_d+U/2|\gg U/2$ [see Appendix B]. This is because in the limit $\epsilon_d\to\infty$ ($\epsilon_d\to-\infty$) the

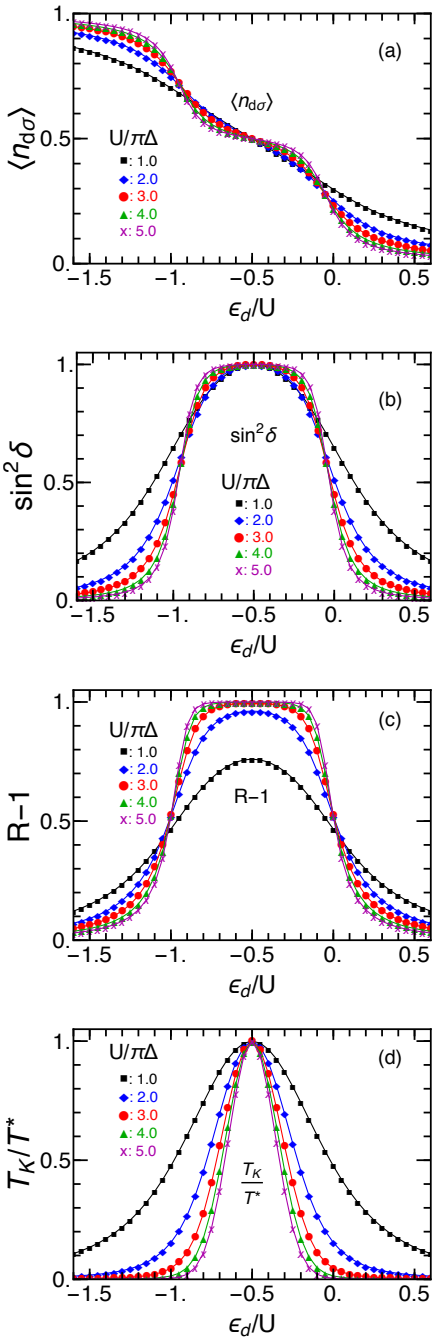

FIG. 2. NRG results for the Fermi-liquid parameters are plotted vs ϵ_d/U, for $U/(\pi\Delta) = 1, 2, 3, 4, 5$. (a) $\langle n_{d\sigma}\rangle$, (b) $\sin^2\delta$, (c) $R-1 = -\chi_{\uparrow\downarrow}/\chi_{\uparrow\uparrow}$, and (d) T_K/T^* for which $T^* \equiv 1/(4\chi_{\uparrow\uparrow})$ depends on ϵ_d/U and T_K is defined as the value of T^* at half-filling $\epsilon_d = -U/2$.

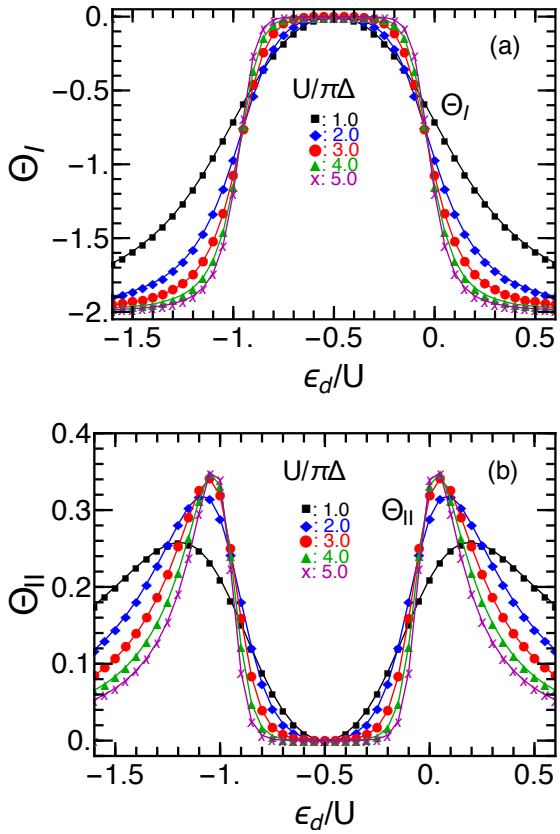

FIG. 3. NRG results for the three-body correlation functions, $\Theta_{\rm I} \equiv \frac{\sin 2\delta}{2\pi\chi^2_{\uparrow\uparrow}}\chi^{[3]}_{\uparrow\uparrow\uparrow}$ and $\Theta_{\rm II} \equiv \frac{\sin 2\delta}{2\pi\chi^2_{\uparrow\uparrow}}\chi^{[3]}_{\uparrow\downarrow\downarrow}$, are plotted vs ϵ_d/U in (a) and (b), respectively, for $U/(\pi\Delta) = 1, 2, 3, 4, 5$.

impurity level is almost empty (fully filled) and effects of the Coulomb interaction become less important.

The results for the three-body correlations $\Theta_{\rm I}$ and $\Theta_{\rm II}$, defined in Eq. (27), are plotted in Fig. 3 as functions of ϵ_d/U for several values of $U/(\pi\Delta)$. These two dimensionless parameters, $\Theta_{\rm I}$ and $\Theta_{\rm II}$, vanish in the particle-hole symmetric case $\epsilon_d = -U/2$, and are suppressed in the wide Kondo regime $-U \lesssim \epsilon_d \lesssim 0$ for large U. At the both ends of this region near $\epsilon_d \simeq 0$ and $-U$, the three-body correlations evolve significantly and play an important role in next-leading order terms of the transport coefficients, i.e. C_T, $C_V^{(2)}$, and $C_V^{(3)}$ in Eq. (25). In particular, $\Theta_{\rm II}$ has a peak in the valence fluctuation regime, which becomes sharper as U increases. Further away from half-filing $|\epsilon_d| \to \infty$, the three-body correlations also approach the noninteracting values $\Theta_{\rm I} \to -2$ and $\Theta_{\rm II} \to 0$ [see Appendix B]. Note that the three-body susceptibility $\chi^{[3]}_{\sigma\sigma'\sigma''}$ itself is an odd function of $\xi_d \equiv \epsilon_d + U/2$. The dimensionless parameters $\Theta_{\rm I}$ and $\Theta_{\rm II}$ become even functions of ξ_d since $\sin 2\delta$ is also an odd function.

V. PROPERTIES OF ORDER $(eV)^2$ NONLINEAR CURRENT

In this section, we examine how the order $(eV)^2$ term of the nonlinear current I varies with gate voltage ϵ_d and Coulomb interaction U in the presence of the tunnel and bias asymmetries.

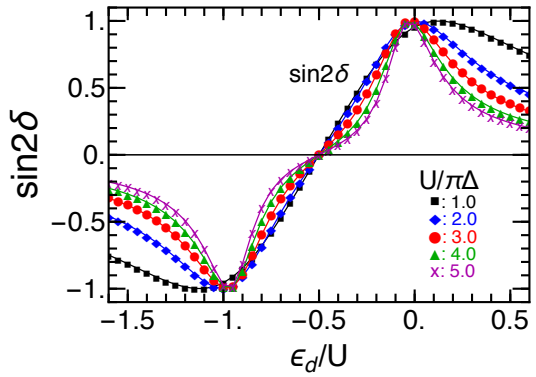

FIG. 4. NRG results for $\sin 2\delta$ are plotted vs ϵ_d/U, for $U/(\pi\Delta) = 1, 2, 3, 4, 5$.

A. General properties of $C_V^{(2)}$

The coefficient defined in Eq. (29) consists of two parts: $C_V^{(2)} = (\pi/4)\left[\overline{C}_V^{(2a)} + \overline{C}_V^{(2b)}\right]\sin 2\delta$ with

$$\overline{C}_V^{(2a)} \equiv \alpha_{\rm dif}\,, \tag{37}$$

$$\overline{C}_V^{(2b)} \equiv -\left(\alpha_{\rm dif} + \frac{\Gamma_L - \Gamma_R}{\Gamma_L + \Gamma_R}\right)(R-1)\,. \tag{38}$$

These two parts represent contributions of ω-linear and eV-linear terms, respectively, of the low-energy expansion of the spectral function $A(\omega, T, eV)$, described in Appendix A.

As shown in Fig. 2 (c), the Wilson ratio has a plateau of the height $R-1 \simeq 1$ in the Kondo regime, i.e. $-U \lesssim \epsilon_d \lesssim 0$ for $U/(\pi\Delta) \gtrsim 2$. Thus, in this region, the coefficient becomes independent of bias asymmetry,

$$C_V^{(2)} \xrightarrow{R-1\to 1} -\frac{\pi}{4}\frac{\Gamma_L - \Gamma_R}{\Gamma_L + \Gamma_R}\sin 2\delta\,. \tag{39}$$

Outside the Kondo regime, especially in the limit of $|\epsilon_d| \to \infty$, the Wilson ratio approaches the noninteracting value $R-1 \to 0$, and the coefficient becomes independent of tunnel asymmetry,

$$C_V^{(2)} \xrightarrow{R-1\to 0} \frac{\pi}{4}\,\alpha_{\rm dif}\,\sin 2\delta\,. \tag{40}$$

The dependence of $C_V^{(2)}$ on impurity level ϵ_d is determined also by the other factor $\sin 2\delta$. It is related to the derivative of the spectral weight at equilibrium $\partial\rho_d/\partial\omega$ as shown in Eq. (28), and vanishes at half-filling where $\delta = \pi/2$. In Fig. 4, the NRG results for $\sin 2\delta$ are plotted vs ϵ_d/U for several values of U. It has a peak at $\delta = \pi/4$ and a dip at $3\pi/4$, which correspond to the level positions for $\epsilon_d \simeq 0$ and $-U$, respectively. For strong interactions $U \gg \Delta$, the peak and dip become sharper as the occupation number $\langle n_{d\sigma}\rangle$ varies abruptly at these two valence fluctuation regions as shown in Fig. 2 (a).

B. Level shift due to bias voltage eV

We next examine how the impurity level evolves at finite bias voltage in the junction with tunnel and bias asymmetries, which affects significantly the nonlinear current of order $(eV)^2$. As $C_V^{(2)}$ is determined by the linear-order terms of the self-energy $\mathrm{Re}\,\Sigma^r(\omega, T, eV)$ with respect to the frequency and bias voltage, we consider the low-energy form of the spectral function which is correct up to terms of order ω and eV,

$$\pi\Delta A^{(1)}(\omega) \equiv \frac{\widetilde{\Delta}^2}{\left(\omega - \widetilde{\epsilon}_d^{(1)}\right)^2 + \widetilde{\Delta}^2}\,, \tag{41}$$

$$\widetilde{\epsilon}_d^{(1)} \equiv \widetilde{\Delta}\cot\delta + \frac{R-1}{2}\left(\alpha_{\rm dif} + \frac{\Gamma_L - \Gamma_R}{\Gamma_L + \Gamma_R}\right)eV\,. \tag{42}$$

Here, $\widetilde{\epsilon}_d^{(1)}$ is the renormalized impurity level that situates at $\widetilde{\Delta}\cot\delta$ for $eV = 0$, with $\widetilde{\Delta} = z\Delta$ the renormalized level width. When a bias voltage eV is applied, it moves upwards or downwards from the equilibrium position depending on sign of the coefficient $\alpha_{\rm dif} + (\Gamma_L - \Gamma_R)/\Delta$. This shift of the impurity level is induced for interacting electrons, and is suppressed as the Wilson ratio approaches the noninteracting value $R-1 \to 0$. Note that the occupation number of the Anderson impurity is determined by the spectral function also at finite eV [66],

$$\langle n_{d\sigma}\rangle = \int_{-\infty}^{\infty} d\omega\, f_{\rm eff}(\omega)\, A(\omega, T, eV)\,, \tag{43}$$

$$f_{\rm eff}(\omega) \equiv \frac{\Gamma_L\, f(\omega - \mu_L) + \Gamma_R f(\omega - \mu_R)}{\Gamma_L + \Gamma_R}\,, \tag{44}$$

and thus $\widetilde{\epsilon}_d^{(1)}$ directly affects charge distribution around quantum dots.

For $\Gamma_L > \Gamma_R$, the number of electrons entering the quantum dot from the source side becomes larger than the number of electrons leaving from the dot towards the drain side. Therefore, the number of electron in the dot increases and the repulsive interaction pushes effective level towards high-energy side. In opposite case, for $\Gamma_L < \Gamma_R$, the effective level moves towards low-energy side. Similarly, the bias symmetry affects the charge distribution. The number of electrons in the dot increases for $(\mu_L + \mu_R)/2 > 0$, namely for $\alpha_{\rm dif} > 0$, and the Coulomb repulsion pushes $\widetilde{\epsilon}_d^{(1)}$ upwards. The number of electrons and $\widetilde{\epsilon}_d^{(1)}$ evolve in the opposite direction for $(\mu_L + \mu_R)/2 < 0$.

Figure 5 demonstrates how $\widetilde{\epsilon}_d^{(1)}$ evolves with bias voltage eV in a junction with tunnel asymmetries $\Gamma_L \neq \Gamma_R$ for a symmetric bias $\alpha_{\rm dif} = 0$, choosing $U/(\pi\Delta) = 4.0$ and $\epsilon_d = -U$. It describes the level shifts occurring in the middle of the valence fluctuation region, and in this case $\widetilde{\epsilon}_d^{(1)} = -0.91\Delta$ at $eV = 0$. The slope of the lines can be steeper for strong repulsions that make $R-1$ larger, and the coefficient $C_V^{(2)}$ is enhanced significantly in such

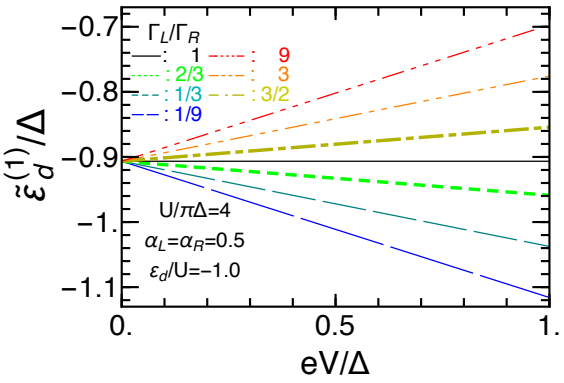

FIG. 5. Effective impurity level $\tilde{\epsilon}_d^{(1)}$ vs eV for a junction with tunnel asymmetries $\Gamma_L/\Gamma_R = 1/9, 1/3, 2/3, 1, 3/2, 3, 9$ for chemical potentials $\mu_L = -\mu_R = eV/2$ ($\alpha_{\rm dif} = 0$). The other parameters chosen to be $U/(\pi\Delta) = 4.0$ and $\epsilon_d = -U$, at which the FL parameters take values $z = 0.75$, $R - 1 = 0.52$, and $\tilde{\epsilon}_d^{(1)} = -0.91\Delta$ at $eV = 0$.

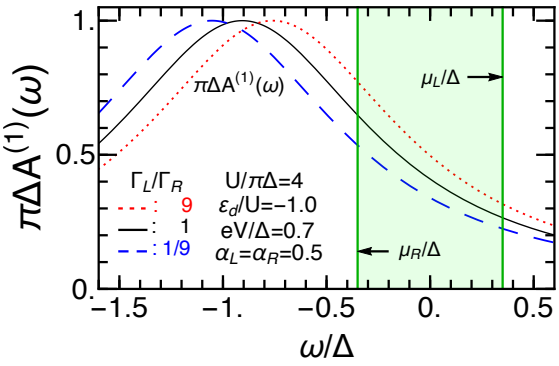

FIG. 6. Behavior of $A^{(1)}(\omega)$ defined in Eq. (41) near the Fermi level for a junction with tunnel asymmetries of $\Gamma_L/\Gamma_R = 1/9$ (dashed line), 1 (solid line), 9 (dotted line). Bias voltage is applied such that $\mu_L = -\mu_R = eV/2$ with $eV = 0.7\Delta$, choosing $U/(\pi\Delta) = 4$ and $\epsilon_d = -U$. The area between the curve for $A^{(1)}(\omega)$ and horizontal axis in the shaded region, which represents the bias window, determines order $(eV)^2$ nonlinear current with the formula Eq. (20).

cases. Figure 6 also demonstrates behavior of $A^{(1)}(\omega)$ near the Fermi level for a junction with tunnel asymmetries $\Gamma_L/\Gamma_R = 1/9, 1, 9$, applying bias voltages such that $\alpha_{\rm dif} = 0$ and $eV = 0.7\Delta$ for the same valence fluctuation state as that examined in Fig. 5. In this example, the spectral peak corresponding to the effective level situates at $\tilde{\epsilon}_d^{(1)} = -0.91\Delta$ for $\Gamma_L = \Gamma_R$, below the bias window $\mu_R \le \omega \le \mu_L$ which is described as a shaded region. When a bias voltage eV is applied to an asymmetric tunnel junction with $\Gamma_L \neq \Gamma_R$, the peak shifts in such a way as the dashed or dotted line in Fig. 6. Simultaneously, the spectral weight in the bias-window region varies, and it yields order $(eV)^2$ term of the nonlinear current I defined in Eq. (20). Especially, shifts of the effective level cause one of the two parts, i.e. $\overline{C}_V^{(2b)}$ defined in Eq. (38), of the order $(eV)^2$ term.

The other part $\overline{C}_V^{(2a)}$ is determined by the ω-linear term of $A^{(1)}(\omega)$, which is renormalized by the differential coefficient $\partial\Sigma^{\rm eq}/\partial\omega$. It contributes to order $(eV)^2$ nonlinear current for $\alpha_{\rm dif} \neq 0$, i.e. when the bias voltage is applied asymmetrically. Thus, the $\overline{C}_V^{(2a)}$ part can also regarded as contributions caused by the shift of the bias window, taking place in the low-frequency region. An alternative interpretation along this line is described in Appendix C.

C. ϵ_d dependence of order $(eV)^2$ current through junctions with tunnel and bias asymmetries

We next examines behavior of $C_V^{(2)}$ over a wide range of the parameter space, especially its dependence on junction asymmetries $(\Gamma_L - \Gamma_R)/\Delta$ and $\alpha_{\rm diff}$, and also the dependence on ϵ_d and U by which the Fermi-liquid parameters $\sin 2\delta$ and $R - 1$ evolve.

1. *Effects of tunnel asymmetries $\Gamma_L \neq \Gamma_R$, at $\alpha_{\rm dif} = 0$*

We first of all consider effects of tunnel asymmetry, choosing bias voltages to be symmetric $\alpha_{\rm dif} = 0$. In this case the coefficient takes the form $C_V^{(2)} \xrightarrow{\alpha_{\rm dif}=0} -(\pi/4)\left[(\Gamma_L - \Gamma_R)/\Delta\right](R-1)\sin 2\delta$. Therefore, while ϵ_d dependence enters through the product $(R-1)\sin 2\delta$, sign and magnitude of $C_V^{(2)}$ are determined also by tunnel asymmetries $(\Gamma_L - \Gamma_R)/\Delta$. In Fig. 7(a), the NRG results of this coefficient are plotted as a function of ϵ_d/U for $U/(\pi\Delta) = 4$, keeping $\Delta = \Gamma_L + \Gamma_R$ unchanged. We see the all the curves for different $\Gamma_L/\Gamma_R = 1/9, 1/3, 2/3, 1, 3/2, 3, 9$ pass through a common single zero-point at $\epsilon_d = -U/2$, where the phase shift takes the value $\delta = \pi/2$ due to the particle-hole symmetry. Over a wide range of gate voltages $-U \lesssim \epsilon_d \lesssim 0$, the ϵ_d dependence of $C_V^{(2)}$ reflects that of $\sin 2\delta$ since the Wilson ratio $R - 1 \simeq 1$ for $U/(\pi\Delta) \gtrsim 2.0$ as shown in Fig. 2(c). Similarly, the peak and dip structures appearing in the valence fluctuation regime near $\epsilon_d \simeq 0$ and $\epsilon_d \simeq -U$ reflect behavior of $\sin 2\delta$ at $\delta = \pi/4$ and $\delta = 3\pi/4$, shown in Fig. 4. These features of order $(eV)^2$ nonlinear current are pronounced as tunnel asymmetry $|\Gamma_L - \Gamma_R|$ increases. For much larger $|\epsilon_d|$, outside of the valence fluctuation regime, $C_V^{(2)}$ rapidly decreases much faster than $\sin 2\delta$ since effects of electron correlations are suppressed $R-1 \simeq 0$ as the impurity level is almost empty or doubly occupied.

In Fig.7(b), the coefficient $C_V^{(2)}$ for largely imbalanced tunnel couplings $\Gamma_L = 9\Gamma_R$ is plotted for several different values of the interaction $U/(\pi\Delta) = 1, 2, 3, 4, 5$. We can see that the peak and dip structures evolve with U and become sharper as U increases, reflecting the behavior of

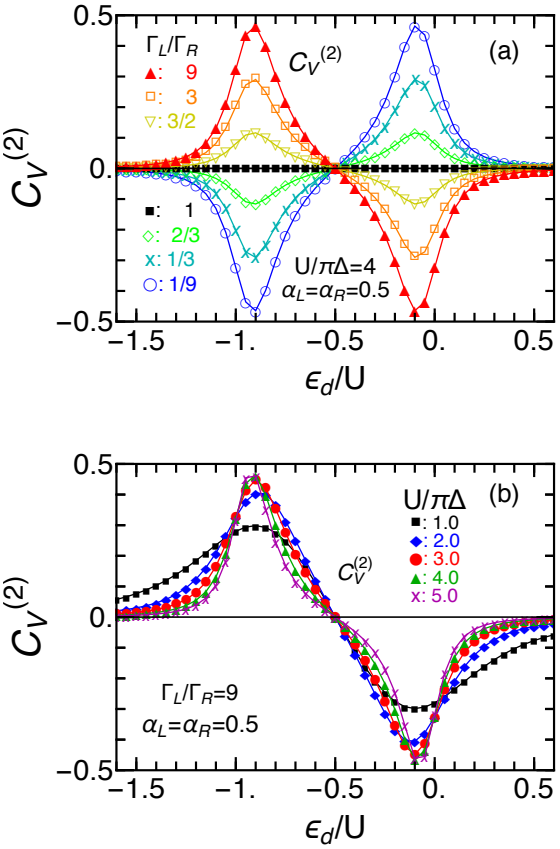

FIG. 7. Top panel (a): NRG results of $C_V^{(2)}$ vs ϵ_d/U for different tunnel asymmetries $\Gamma_L/\Gamma_R = 1/9(\circ)$, $1/3(\times)$, $2/3(\diamond)$, $1(\blacksquare)$, $3/2(\triangledown)$, $3(\square)$, $9(\blacktriangle)$ for $U/(\pi\Delta) = 4.0$, keeping $\Delta = \Gamma_L + \Gamma_R$ unchanged. Bottom panel (b): $C_V^{(2)}$ for several values of interactions $U/(\pi\Delta) = 1, 2, 3, 4, 5$, for fixed tunnel couplings $\Gamma_L = 9\Gamma_R$. For both (a) and (b), bias voltages are chosen to be symmetric $\alpha_L = \alpha_R = 1/2$, i.e. $\alpha_{\rm dif} = 0$.

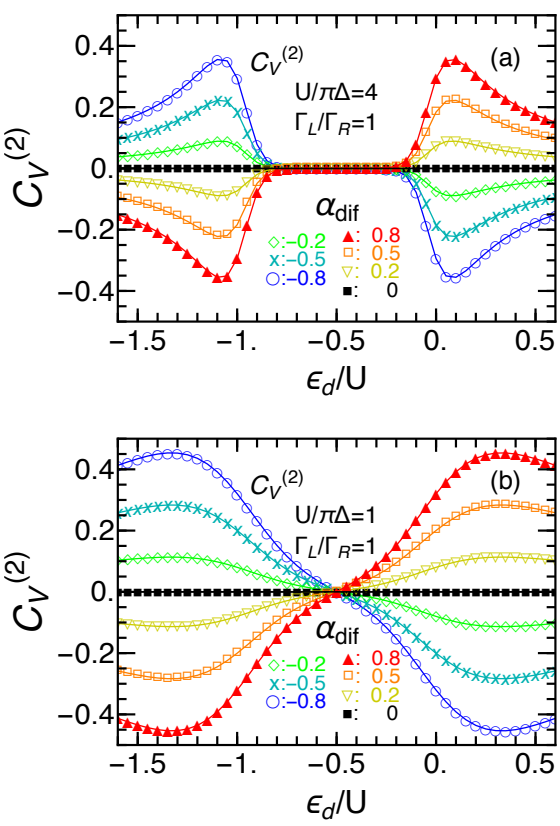

FIG. 8. NRG results of $C_V^{(2)}$ for symmetric tunnel couplings with $\Gamma_L = \Gamma_R$ are plotted for different degrees of bias asymmetries $\alpha_{\rm dif} = -0.8(\circ)$, $-0.5(\times)$, $-0.2(\diamond)$, $0.0(\blacksquare)$, $0.2(\triangledown)$, $0.5(\square)$, $0.8(\blacktriangle)$. Coulomb interactions are chosen to be (a) $U = 4\pi\Delta$, and (b) $U = \pi\Delta$.

$\sin 2\delta$ shown in Fig. 4. Furthermore, $C_V^{(2)}$ is suppressed in the Kondo regime $-U \lesssim \epsilon_d \lesssim 0$ for strong interactions.

2. *Effects of bias asymmetries $\alpha_{\rm dif} \neq 0$, at $\Gamma_L = \Gamma_R$*

We next consider effects caused by shift of the bias window which occurs for $\alpha_L \neq \alpha_R$ ($\alpha_{\rm dif} \neq 0$). For this purpose, we assume here the tunnel couplings to be symmetric $\Gamma_L = \Gamma_R$. In this case, the coefficient takes the form $C_V^{(2)} \xrightarrow{\Gamma_L=\Gamma_R} (\pi/4)\,\alpha_{\rm dif}\,(2-R)\,\sin 2\delta$, and thus the ϵ_d dependence is determined by the product $(2-R)\,\sin 2\delta$ while sign and magnitude vary with bias asymmetries $\alpha_{\rm dif}$. Note that the factor $2-R$ is proportional to the charge susceptibility χ_c defined at $T = 0$, and it can be written in the following form using Eq. (18),

$$\chi_c \equiv -\sum_\sigma \frac{\partial\langle n_{d\sigma}\rangle}{\partial\epsilon_d} = 2\left(\chi_{\uparrow\uparrow} + \chi_{\uparrow\downarrow}\right) = \frac{2-R}{2T^*}. \quad (45)$$

In Fig. 8, the NRG results of $C_V^{(2)}$ for this case are plotted vs ϵ_d for different degrees of bias asymmetries $\alpha_{\rm dif} = -0.8, -0.5, -0.2, 0, 0.2, 0.5, 0.8$, choosing two different Coulomb repulsions (a) $U/(\pi\Delta) = 4$ and (b) $U/(\pi\Delta) = 1$. For strong interactions, order $(eV)^2$ component of the nonlinear current vanishes $C_V^{(2)} \simeq 0$ over a wide region $-U \lesssim \epsilon_d \lesssim 0$, as seen in Fig. 8(a). This is because the charge fluctuations are suppressed and thus $\chi_c \propto 2-R \simeq 0$ in the Kondo regime. However, as demonstrated in Fig. 8(b), $C_V^{(2)}$ takes finite values for weak interactions because the charge excitations occurring near the quantum dot are still active for $U/(\pi\Delta) \lesssim 2.0$, as it can be deduced from the behavior of $R-1$ shown in Fig. 2(c). The peak and dip structures seen in the valence fluctuation regime near $\epsilon_d \simeq 0$ and $\epsilon_d \simeq -U$ reflect the behavior of $\sin 2\delta$ at $\delta = \pi/4$ and $\delta = 3\pi/4$, similarly to those observed for the symmetric bias case in Fig. 7. $C_V^{(2)}$ vanishes when both the tunnel and bias asymmetries are absent, i.e. at $\Gamma_L = \Gamma_R$ and $\alpha_{\rm dif} = 0$, as mentioned.

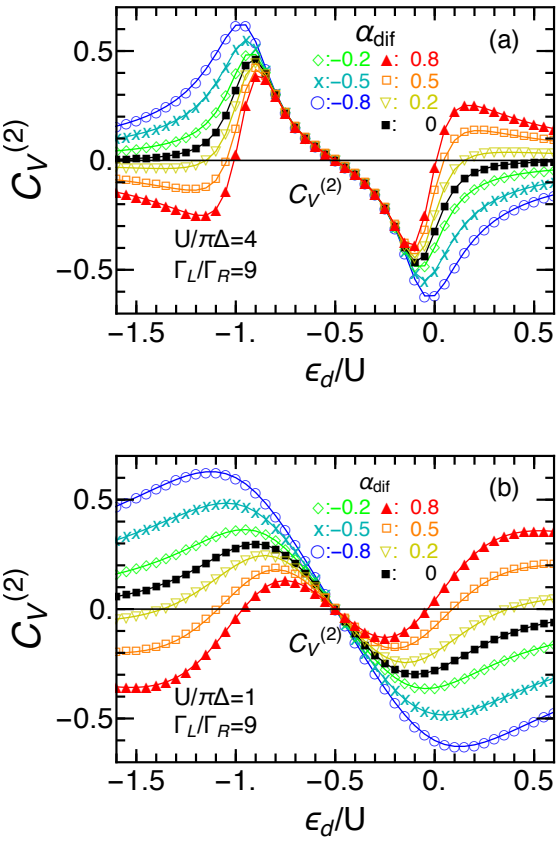

FIG. 9. NRG results of $C_V^{(2)}$ for junctions with large imbalanced couplings $\Gamma_L = 9\Gamma_R$ are plotted for different degrees of bias asymmetries $\alpha_{\rm dif} = -0.8(\circ)$, $-0.5(\times)$, $-0.2(\diamond)$, $0.0(\blacksquare)$, $0.2(\triangledown)$, $0.5(\square)$, $0.8(\blacktriangle)$. Coulomb interactions are chosen to be (a) $U = 4\pi\Delta$, and (b) $U = \pi\Delta$.

3. *Effects of bias asymmetries $\alpha_{\rm dif} \neq 0$, for junctions with largely imbalanced couplings $\Gamma_L \gg \Gamma_R$*

So far, we have examined separately effects of tunnel asymmetry and bias asymmetry which enter through the parameters Γ_L/Γ_R and $\alpha_{\rm dif}$, respectively, assuming that perturbations due to one of these two asymmetries is absent. We next consider behavior of the order $(eV)^2$ nonlinear response in the situation where both of these asymmetries are present. In particular, for junctions with largely imbalanced tunnel couplings $\Gamma_L \gg \Gamma_R$, specifically for $\Gamma_L = 9\Gamma_R$.

In Fig. 9, the coefficient $C_V^{(2)}$ is plotted for different degrees of bias asymmetries $\alpha_{\rm dif} = -0.8$, -0.5, -0.2, 0.0, 0.2, 0.5, 0.8, choosing interactions to be (a) $U = 4\pi\Delta$ and (b) $U = \pi\Delta$. One of the lines in Fig. 9 (a) plotted for $\alpha_{\rm dif} = 0$ is identical to the line for $\Gamma_L = 9\Gamma_R$ in Fig. 7 (a). We can see that $C_V^{(2)}$ for strong interactions $U = 4\pi\Delta$ is not affected by the bias asymmetries $\alpha_{\rm dif}$ over the wide region $-U \lesssim \epsilon_d \lesssim 0$, where the Wilson ratio approaches $R - 1 \simeq 1$ and $C_V^{(2)}$ can be expressed in the form of Eq. (39). The coefficient $C_V^{(2)}$ captures two extra zero-points for $\alpha_{\rm dif} > 0$ in the valence fluctuation region, at $\epsilon_d \simeq -U$ and $\epsilon_d \simeq 0$. It happens at the points where the two contributions defined in Eqs. (37) and (38) cancel each other out $\overline{C}_V^{(2a)} + \overline{C}_V^{(2b)} = 0$. This condition that determines the values of ϵ_d at the extra zero-points can also be expressed in the form,

$$R - 1 = \frac{\alpha_{\rm dif}}{\alpha_{\rm dif} + \frac{\Gamma_L - \Gamma_R}{\Gamma_L + \Gamma_R}}, \tag{46}$$

and it has a solution if $(\Gamma_L - \Gamma_R)\,\alpha_{\rm dif} > 0$ as the Wilson ratio takes a value in the range $0 \leq R - 1 \leq 1$. The extra zero-points move towards high-energy side as $\alpha_{\rm dif}$ approaches zero. Note that the contributions of $\overline{C}_V^{(2a)}$ and $\overline{C}_V^{(2b)}$ parts are caused by shift of the bias window and that of the effective level $\widetilde{\epsilon}_d^{(1)}$, respectively, as shown in Appendix C. For $(\Gamma_L - \Gamma_R)\,\alpha_{\rm dif} < 0$, we can also see in Fig. 9 (a) that these two contributions become cooperative and $C_V^{(2)}$ is enhanced significantly in the valence fluctuation regime.

Outside of the Kondo and valence fluctuation regimes $|\epsilon_d + U/2| \gg U/2$, the magnitude of $C_V^{(2)}$ becomes independent of tunnel asymmetries and is proportional to $\alpha_{\rm dif}$ obeying Eq. (40). Thus, as $|\epsilon_d|$ increases, behaviors of the curves in Fig. 9 (a) approach that of the curves for the same $\alpha_{\rm dif}$ shown in Fig. 8 (a) for the $\Gamma_L = \Gamma_R$ case. For weak interactions $U/(\pi\Delta) \lesssim 2.0$, charge fluctuations contribute to low-energy transport also near half-filling $\epsilon_d \simeq -U/2$, as seen in Fig. 2. It causes variations in $C_V^{(2)}$ seen whole regions of ϵ_d in Fig. 9 (b) against $\alpha_{\rm dif}$. The behaviors in the case of the opposite tunnel asymmetries, for which Γ_L is much smaller than Γ_R, can also be deduced from the results shown in Fig. 9, specifically for $\Gamma_L = \Gamma_R/9$, using the relation $C_V^{(2)}(\alpha_{\rm dif}, \Gamma_L/\Gamma_R) = -C_V^{(2)}(-\alpha_{\rm dif}, \Gamma_R/\Gamma_L)$ given in Eq. (34).

4. *Effects of tunnel asymmetries $\Gamma_L \neq \Gamma_R$, for junctions with a maximized bias asymmetry $\alpha_{\rm dif} = 1$*

We also examine the situation where the electrode of drain side is grounded, choosing the parameters such that $\alpha_L = 1$ and $\alpha_R = 0$, i.e. $\alpha_{\rm dif} = 1$. This corresponds to one typical situation occurring in real measurements. In this case, the coefficient takes the form $C_V^{(2)} \xrightarrow{\alpha_{\rm dif}=1} (\pi/4)\,[1 - 2\,(R-1)\,\Gamma_L/\Delta]\sin 2\delta$. The NRG results are shown in Fig. 10.

In Fig. 10(a), the coefficient $C_V^{(2)}$ in this case $\alpha_{\rm dif} = 1$ is plotted for seven different tunnel asymmetries $\Gamma_L/\Gamma_R = 1/9$, $1/3$, $2/3$, 1, $3/2$, 3, 9, choosing $U = 4\pi\Delta$ at which the Wilson ratio is almost saturated to the strong coupling value $R - 1 \simeq 1$ in the Kondo regime, as mentioned. Therefore, $C_V^{(2)}$ varies with Γ_L/Γ_R for $-U \lesssim \epsilon_d \lesssim 0$, obeying Eq. (39). It also has two extra zero-points for

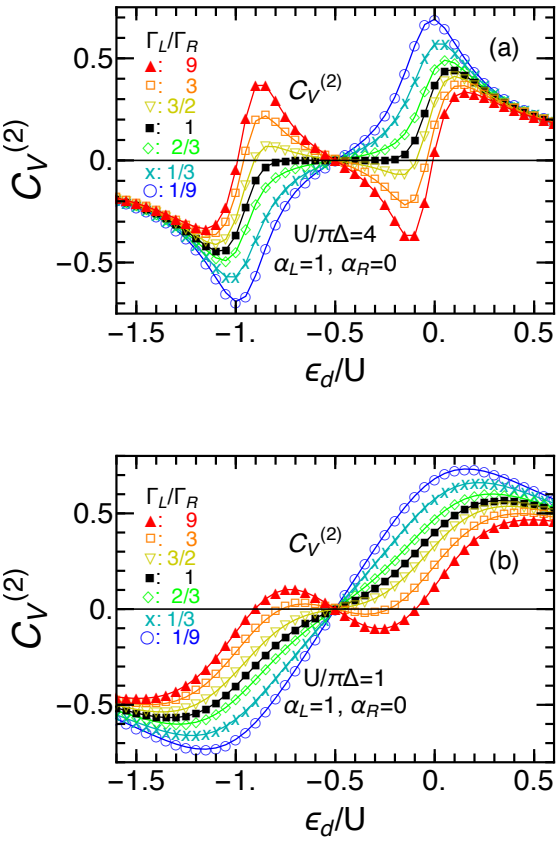

FIG. 10. NRG results of $C_V^{(2)}$ for a maximized bias asymmetry $\alpha_L = 1$ and $\alpha_R = 0$ (i.e. $\mu_L = eV$ and $\mu_R = 0$) for different degrees of tunnel asymmetries $\Gamma_L/\Gamma_R = 1/9(\circ)$, $1/3(\times)$, $2/3(\diamond)$, $1(\blacksquare)$, $3/2(\triangledown)$, $3(\square)$, $9(\blacktriangle)$, for a fixed Coulomb interaction $U/(\pi\Delta) = 4$. Coulomb interactions are chosen to be (a) $U = 4\pi\Delta$, and (b) $U = \pi\Delta$.

$(\Gamma_L - \Gamma_R)\,\alpha_{\rm dif} > 0$ in the valence fluctuation region as a result of the cancellation of the $\overline{C}_V^{(2a)}$ and $\overline{C}_V^{(2b)}$ components, described in Eq. (46). Similarly, these two components become cooperative for the opposite cases where $(\Gamma_L - \Gamma_R)\,\alpha_{\rm dif} < 0$, and it enhances largely the order $(eV)^2$ nonlinear current. For much larger $|\epsilon_d|$, all the data collapse into a single curve as the coefficient $C_V^{(2)}$ becomes independent of tunnel asymmetries, which can be explained with Eq. (40).

The coefficient $C_V^{(2)}$ for a weak interaction $U = \pi\Delta$ is in Fig. 10 (b), keeping the other parameters are the same as those used for (a). All the curve for different Γ_L/Γ_R become moderate as charge fluctuations of electrons in quantum dots contribute to low-energy transport whole regions of ϵ_d. We see that $C_V^{(2)}$ for the cases $(\Gamma_L - \Gamma_R)\,\alpha_{\rm dif} < 0$ where the tunnel and bias asymmetries are cooperative are enhanced significantly, especially for $\Gamma_L/\Gamma_R = 1/9$.

VI. PROPERTIES OF ORDER $(eV)^3$ NONLINEAR CURRENT

In this section, we study effects of tunnel and bias asymmetries on the order $(eV)^3$ nonlinear current. The coefficient for this component in dI/dV consists of two parts: $C_V^{(3)} = (\pi^2/64)(W_V + \Theta_V)$ with the two-body W_V and three-body Θ_V contributions defined in Eqs. (30)–(32). One of the important properties deduced from these formulas, summarized also in Table I, is that effects of tunnel asymmetries enter into W_V and Θ_V through the cross term of $\Gamma_L - \Gamma_R$ and $\alpha_{\rm dif}$ of the form,

$$\frac{\Gamma_L - \Gamma_R}{\Gamma_L + \Gamma_R}\,\alpha_{\rm dif}\,. \tag{47}$$

Thus, for symmetrical bias voltages $\alpha_{\rm dif} = 0$, the coefficient $C_V^{(3)}$ is not affected by tunnel asymmetries.

From the formulas in Table I, some general properties of $C_V^{(3)}$ can also be deduced for the three characteristic regions of a wide parameter space for quantum dots, i.e. the Kondo regime, valence fluctuation regime, and empty (fully-occupied)-orbital regime for $|\epsilon_d| \to \infty$.

In the Kondo regime at $-U \lesssim \epsilon_d \lesssim 0$ and $U/(\pi\Delta) \gtrsim 2$, most of the Fermi-liquid parameters take constant values as shown in Figs. 2 and 3: $\delta \simeq \pi/2$, $R - 1 \simeq 1$, and three-body correlations almost vanish $\Theta_{\rm I} \simeq 0$ and $\Theta_{\rm II} \simeq 0$. Therefore, over a wide parameter region of the Kondo regime, $C_V^{(3)}$ becomes almost independent of tunnel and bias asymmetries, as

$$W_V \xrightarrow{\text{Kondo regime}} 6\,, \qquad \Theta_V \xrightarrow{\text{Kondo regime}} 0\,. \tag{48}$$

In the valence fluctuation regime at $\epsilon_d \simeq 0$ and $-U$, the cosine factor passes through the zero-point as $\cos 2\delta = 0$ at $\delta = \pi/4$ and $3\pi/4$, corresponding to $1/4$ and $3/4$ fillings. Therefore, near these zero-points, the two-body part W_V is suppressed and the three-body part Θ_V gives important contributions in the valence fluctuation regime.

Outside these regions, in the limit of $|\epsilon_d| \to \infty$, the impurity level approaches empty or fully occupied, and the FL parameters asymptotically take noninteracting values, i.e. $\cos 2\delta \simeq 1$, $R - 1 \simeq 0$, $\Theta_{\rm I} \simeq -2$, $\Theta_{\rm II} \simeq 0$, as shown in Appendix B. Thus, the two-body W_V and three-body Θ_V parts are given by

$$\begin{aligned} W_V &\xrightarrow{|\epsilon_d|\to\infty} -\Big(1 + 3\,\alpha_{\rm dif}^2\Big), \\ \Theta_V &\xrightarrow{|\epsilon_d|\to\infty} -2\Big(1 + 3\,\alpha_{\rm dif}^2\Big). \end{aligned} \tag{49}$$

Note that $C_V^{(3)}$ becomes independent of tunnel asymmetries in this limit.

A. $C_V^{(3)}$ for symmetric bias: $\alpha_L = \alpha_R = 1/2$ ($\alpha_{\rm dif} = 0$)

We next consider the case where bias voltages are applied symmetrically, i.e. $\alpha_{\rm dif} = 0$. In this case, $C_V^{(3)}$ takes

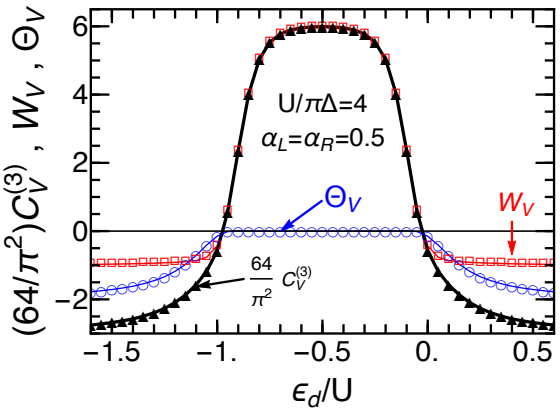

FIG. 11. NRG results of the coefficient for order $(eV)^3$ nonlinear current $C_V^{(3)} = (\pi^2/64)(W_V + \Theta_V)$ are plotted vs ϵ_d/U for a symmetric bias $\alpha_L = \alpha_R = 1/2$, choosing $U/(\pi\Delta) = 4$. In this case $\alpha_{\rm dif} = 0$, the both two-body W_V and three-body Θ_V contributions become independent of tunnel asymmetries $(\Gamma_L - \Gamma_R)/\Delta$ from the definition summarized in Table I.

the following form and becomes independent of the tunnel asymmetry as mentioned,

$$W_V \xrightarrow{\alpha_{\rm dif}=0} -\Big[\,1 + 5(R-1)^2\,\Big]\cos 2\delta\,, \qquad (50)$$

$$\Theta_V \xrightarrow{\alpha_{\rm dif}=0} \Theta_{\rm I} + 3\,\Theta_{\rm II}\,. \qquad (51)$$

Figure 11 shows the NRG results of $C_V^{(3)}$, W_V and Θ_V in this case $\alpha_{\rm dif} = 0$. The Coulomb repulsion is chosen to be strong $U/(\pi\Delta) = 4$. The coefficient $C_V^{(3)}$ has a broad peak in the Kondo regime, and it is determined by the two-body contributions W_V since $\Theta_V \simeq 0$ over the range of $-U \lesssim \epsilon_d \lesssim 0$ as both of the three-body components $\Theta_{\rm I}$ and $\Theta_{\rm II}$ almost vanish in this region, as shown in Fig. 3. The coefficient $C_V^{(3)}$ decreases rapidly in the valence fluctuation regime at $\epsilon_d \simeq 0$ and $\epsilon_d \simeq -U$. As $|\epsilon_d|$ increases further, the two- and three-body components give comparable contributions, and approach $W_V \to -1$ and $\Theta_V \to -2$ in the limit of $|\epsilon_d| \to \infty$. Thus, $(64/\pi^2)\,C_V^{(3)} \xrightarrow{|\epsilon_d|\to\infty} -3$.

B. $C_V^{(3)}$ for asymmetric bias: $\alpha_L \neq \alpha_R$ ($\alpha_{\rm dif} \neq 0$)

We next examine effects of bias asymmetries $\alpha_L \neq \alpha_R$. In this case, the coefficient $C_V^{(3)}$ for order $(eV)^3$ nonlinear current depends on tunnel asymmetries through the cross term $\alpha_{\rm dif}\,(\Gamma_L - \Gamma_R)/\Delta$ described in Eq. (47).

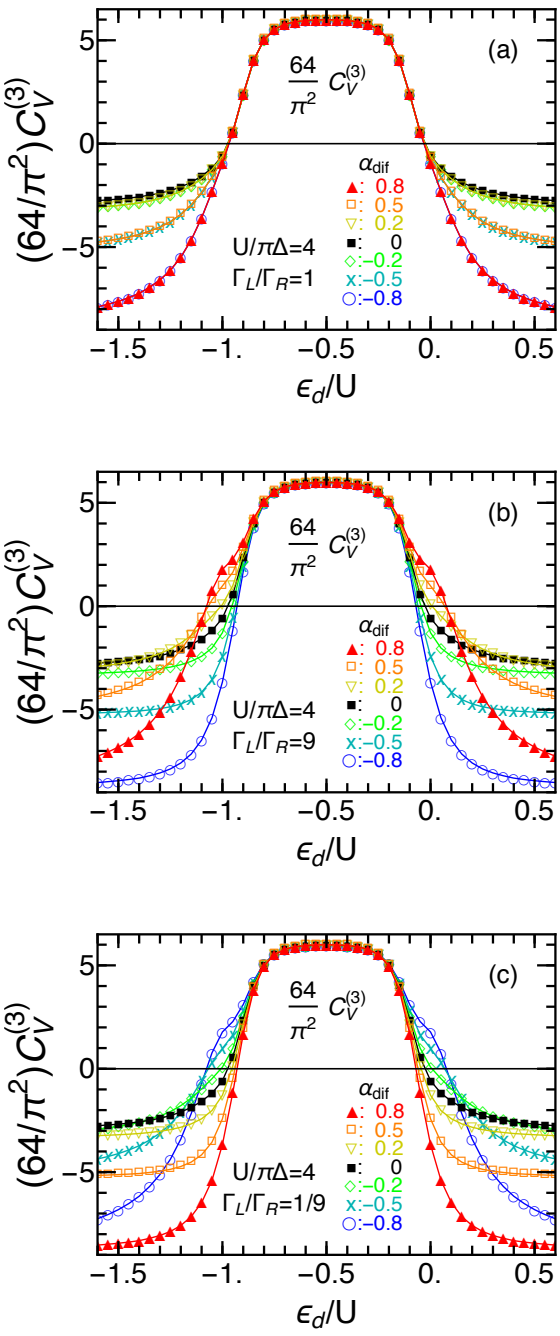

FIG. 12. $C_V^{(3)}$ for $\alpha_{\rm dif} = -0.8(\circ)$, $-0.5(\times)$, $-0.2(\diamond)$, $0.0(\blacksquare)$, $0.2(\triangledown)$, $0.5(\square)$, $0.8(\blacktriangle)$ are plotted for three different tunnel couplings (a) $\Gamma_L = \Gamma_R$, (b) $\Gamma_L/\Gamma_R = 9$, and (c) $\Gamma_L/\Gamma_R = 1/9$, choosing the interaction to be $U/(\pi\Delta) = 4$.

1. *Effects of bias asymmetries ($\alpha_{\rm dif} \neq 0$) on $C_V^{(3)}$ for different degrees of tunnel asymmetries*

In Fig. 12, the coefficient $C_V^{(3)}$ is plotted for different degrees of bias asymmetries $\alpha_{\rm dif} = -0.8, -0.5, -0.2, 0.0, 0.2, 0.5, 0.8$, for strong Coulomb repulsion $U = 4\pi\Delta$.

Three panels (a), (b) and (c) correspond to the results obtained for different tunnel couplings: (a) symmetric one $\Gamma_L = \Gamma_R$, and two largely imbalanced tunnel couplings (b) $\Gamma_L = 9\Gamma_R$ and (c) $\Gamma_L = \Gamma_R/9$. Note that there is a relation between these curves against the inversion of (α_L, Γ_L) and (α_R, Γ_R): $C_V^{(3)}(\alpha_{\rm dif}, \Gamma_L/\Gamma_R) = C_V^{(3)}(-\alpha_{\rm dif}, \Gamma_R/\Gamma_L)$, as shown in Eq. (35).

In the Kondo regime $-U \lesssim \epsilon_d \lesssim 0$, the coefficient $C_V^{(3)}$ is not affected by tunnel or bias asymmetries and has a wide plateau of the height $(64/\pi^2)C_V^{(3)} \simeq 6.0$ given in Eq. (48). Outside the plateau region, the coefficient $C_V^{(3)}$ varies with $\alpha_{\rm dif}$ and asymptotically approaches the saturation value $(64/\pi^2)C_V^{(3)} \xrightarrow{|\epsilon_d|\to\infty} -3\big(1+3\alpha_{\rm dif}^2\big)$ given in Eq. (49) for the empty and fully-occupied orbital regimes. However, for instance in Fig. 12 (b), while the curve for $\alpha_{\rm dif} = -0.8$ approaches very closely to the saturation value -8.76 at the both ends of the horizontal axes $\epsilon_d = -1.6$ and 0.6, the curve for $\alpha_{\rm dif} = 0.8$ still deviates from the saturation value at these points. This is caused by a shoulder structure seen for the curve for $\alpha_{\rm dif} = 0.8$ at $\epsilon_d \simeq -U$ and $\epsilon_d \simeq 0$ in the valence fluctuation regime. The same shoulder structure emerges in the situation where the parameters (α_L, Γ_L) and (α_R, Γ_R) are inverted, i.e. the curve for $\alpha_{\rm dif} = -0.8$ in Fig. 12 (c). This structure is caused by an enhanced contributions of the three-body component $\Theta_{\rm II}$ which has the characteristic peaks that evolve with U in the valence fluctuation regions as seen in Fig. 3 (b). The shoulder structure emerges in the case where the cross term of tunnel and bias asymmetries, $12\alpha_{\rm dif}\,(\Gamma_L - \Gamma_R)/\Delta$, in the formula for Θ_V given in Eq. (32) becomes positive and large. We will discuss contributions of Θ_V more precisely below.

2. *Effects of tunnel asymmetries on $C_V^{(3)}$ for junctions with a maximized bias asymmetry $\alpha_{\rm dif} = 1$*

We next examine effects of tunnel asymmetries for junctions with a maximized bias asymmetry, i.e. the case where bias voltage is applied to the source side keeping the drain grounded $\mu_L = eV$ and $\mu_R = 0$. In this case $\alpha_{\rm dif} = 1$, and the coefficient $C_V^{(3)}$ takes the following form,

$$W_V \xrightarrow{\alpha_{\rm dif}=1} -2\cos 2\delta\left[2 - 3\left(1+\frac{\Gamma_L-\Gamma_R}{\Gamma_L+\Gamma_R}\right)(R-1) + \left(4+3\,\frac{\Gamma_L-\Gamma_R}{\Gamma_L+\Gamma_R}\right)(R-1)^2\right],$$
$$\Theta_V \xrightarrow{\alpha_{\rm dif}=1} 4\,\Theta_{\rm I} + 12\left(1+\frac{\Gamma_L-\Gamma_R}{\Gamma_L+\Gamma_R}\right)\Theta_{\rm II}\,. \qquad (52)$$

The last line shows that the contributions of $\Theta_{\rm II}$ increase with tunnel asymmetries $(\Gamma_L - \Gamma_R)/\Delta$. The two-body part W_V also depends on $(\Gamma_L - \Gamma_R)/\Delta$, However, since another factor $\cos 2\delta$ has a zero-point in the valence fluctuation regions, W_V becomes less sensitive to tunnel asymmetries.

In Fig. 13 (a), the coefficient $C_V^{(3)}$ in this case $\alpha_{\rm dif} = 1$ is plotted for seven different degrees of tunnel couplings $\Gamma_L/\Gamma_R = 1/9,\ 1/3,\ 2/3,\ 1,\ 3/2,\ 3,\ 9$, choosing interactions to be $U/(\pi\Delta) = 4$, keeping $\Delta = \Gamma_L + \Gamma_R$ unchanged. It clearly shows that the shoulder structure evolves in the valence fluctuation regime at $\epsilon_d \simeq -U$ and $\epsilon_d \simeq 0$ as Γ_L/Γ_R, or equivalently $(\Gamma_L - \Gamma_R)/\Delta$, increases. The shoulder structure makes the convergence of $C_V^{(3)}$ at $|\epsilon_d| \to \infty$ protracted, which in this case approaches $C_V^{(3)} \to -12$. As mentioned for this structure appeared in Fig. 12 (b), it occurs when the cross term described in Eq. (47), or the corresponding coefficient for $\Theta_{\rm II}$ in Eq. (52), is positive $\alpha_{\rm dif}\,(\Gamma_L - \Gamma_R)/\Delta > 0$ and large.

The contributions of W_V and Θ_V are also shown separately in Fig. 13, for (b) $\Gamma_L = 9\Gamma_R$, and (c) $\Gamma_L = \Gamma_R/9$, i.e. for two opposite largely imbalanced tunnel asymmetries. The two-body contributions W_V dominate $C_V^{(3)}$ in the Kondo regime as the both three-body components $\Theta_{\rm I}$ and $\Theta_{\rm II}$ almost vanish for $-U \lesssim \epsilon_d \lesssim 0$, similarly to that in the symmetric bias case Fig, 11. In the valence fluctuation regime, the shoulder structure emerges when $\alpha_{\rm dif}\,(\Gamma_L - \Gamma_R)/\Delta$ is large and positive. These two examples show that the two-body part W_V is less sensitive to tunnel asymmetries, i.e. to whether $\Gamma_L = 9\Gamma_R$ or $\Gamma_L = \Gamma_R/9$. In contrast, the three-body part Θ_V has a peak that causes the shoulder structure of $C_V^{(3)}$ in Fig. 13 (b) for which the cross term $\alpha_{\rm dif}(\Gamma_L - \Gamma_R)/\Delta$ is positive and large, whereas it is negative in (c) and $\Theta_{\rm V}$ decreases monotonically as ϵ_d deviates from the particle-hole symmetric point $\epsilon_d = -U/2$.

In Fig. 14, the coefficient $C_V^{(3)}$ is plotted for different values of interactions $U/(\pi\Delta) = 1, 2, 3, 4, 5$, for the same bias asymmetries $\alpha_{\rm dif} = 1$, choosing tunnel couplings to be $\Gamma_L = 9\Gamma_R$. The lower panel (b) shows an enlarged view of the shaded region in (a). The Kondo ridge of $C_V^{(3)}$ becomes flat for strong interactions $U/(\pi\Delta) \gtrsim 3.0$. Simultaneously, the shoulder structure evolves in the valence fluctuation regime at $\epsilon_d \simeq -U$ and $\epsilon_d \simeq 0$ as U increases. It reflects the peak of the three-body correlation $\Theta_{\rm II}$, the height of which increases with U as shown in Fig. 3 (b). These observations show that contributions of $\Theta_{\rm II}$ can be enhanced selectively by tuning tunnel and bias asymmetries to make the cross term $\alpha_{\rm dif}(\Gamma_L - \Gamma_R)/\Delta$ positive and large. Conversely, it also indicates that from measurements of the shoulder structure information about the nonlinear susceptibilities between different spins $\chi^{[3]}_{\uparrow\downarrow\downarrow} \propto \Theta_{\rm II}$ can be extracted.

VII. SUMMARY

In summary, we have studied effects of tunnel and bias asymmetries on the nonlinear current through quantum dots in the low-energy Fermi-liquid regime. We have de-

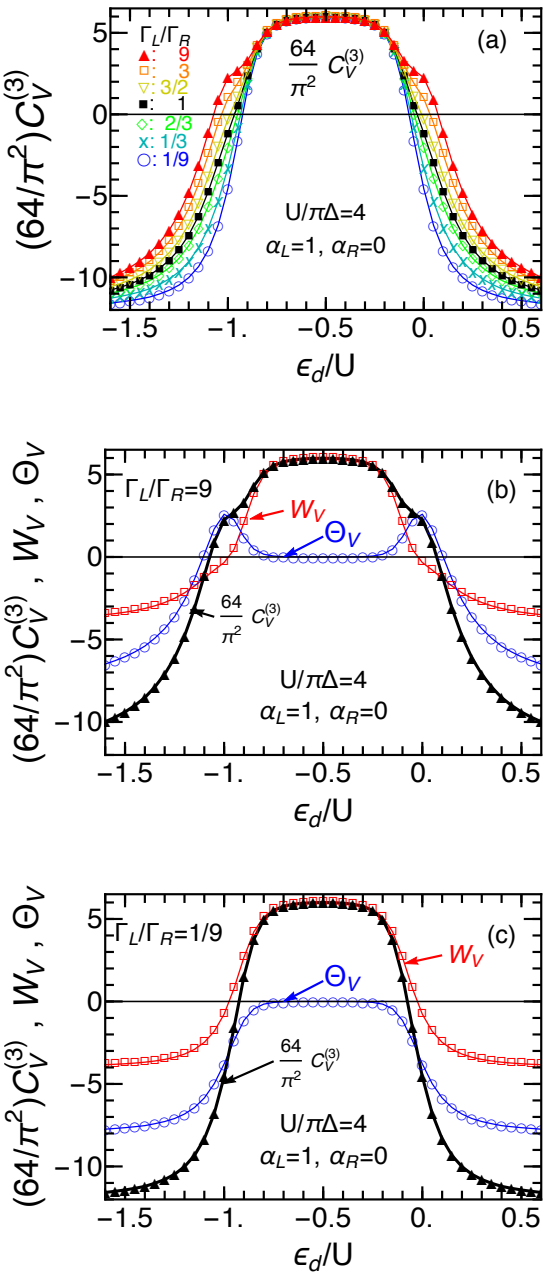

FIG. 13. $C_V^{(3)}$ for a maximized bias asymmetry $\alpha_{\rm dif} = 1$ ($\mu_L = eV$ and $\mu_R = 0$). Top panel (a): different degrees of tunnel asymmetries are examined, taking $\Gamma_L/\Gamma_R = 1/9(\circ)$, $1/3(\times)$, $2/3(\diamond)$, $1(\blacksquare)$, $3/2(\triangledown)$, $3(\square)$, $9(\blacktriangle)$. Middle and bottom panels: W_V and Θ_V are plotted together with $C_V^{(3)}$ for (b) $\Gamma_L = 9\Gamma_R$ and (c) $\Gamma_L = \Gamma_R/9$. The Coulomb interaction is chosen to be $U/(\pi\Delta) = 4$.

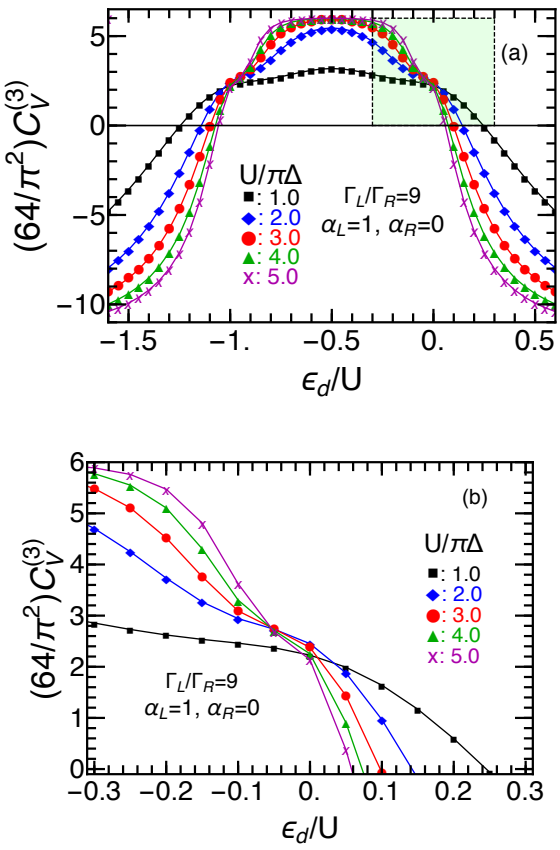

FIG. 14. $C_V^{(3)}$ for $\alpha_{\rm dif} = 1$ and $\Gamma_L/\Gamma_R = 9$ is plotted for different values of Coulomb interactions $U/(\pi\Delta) = 1, 2, 3, 4, 5$. The lower panel (b) shows an enlarged view of the shaded region in (a), describing an evolution of the shoulder structure in the valence fluctuation regime.

rived the generic formula for the differential conductance through the Anderson impurity at $T = 0$ up to terms of order $(eV)^3$, using the exact results for low-energy asymptotic form of the retarded self-energy.

The formula, which is summarized in Table I, explicitly reveal the fact that the Coulomb interaction induces an extra dependence for dI/dV on tunnel asymmetries other than that enters through the prefactor $g_0 = (2e^2/h)\, 4\Gamma_L\Gamma_R/(\Gamma_L+\Gamma_R)^2$. We have also examined behavior of the coefficients $C_V^{(2)}$ and $C_V^{(3)}$ for the nonlinear components of dI/dV using the NRG over a wide range of the parameter space, varying degrees of tunnel and bias asymmetries, and relative position of the impurity level ϵ_d from the Fermi level, for weak and strong interactions U.

Order $(eV)^2$ component of the nonlinear current appears away from half-filling $\epsilon_d \neq -U/2$ when the system has tunnel or bias asymmetries, i.e. $\Gamma_L \neq \Gamma_R$ or $\alpha_{\rm dif} \neq 0$ It reflects the shift of the impurity level of order eV and position of the bias window relative to the Fermi level at equilibrium. In the Kondo regime at $-U \lesssim \epsilon_d \lesssim 0$ for strong interactions $U/(\pi\Delta) \gtrsim 2.0$, the coefficient $C_V^{(2)}$ does not depend on bias asymmetries $\alpha_{\rm dif}$ but on tunnel asymmetries $(\Gamma_L - \Gamma_R)/\Delta$. The coefficient $C_V^{(2)}$ is enhanced especially in the valence fluctuation regime at $\epsilon_d \simeq 0$ and $\epsilon_d \simeq -U$. In the case where sign of $\alpha_{\rm dif}$ and that of $(\Gamma_L - \Gamma_R)/\Delta$ are the same, the tunnel and

bias asymmetries tend to cancel their effects in the valence fluctuation regime, and it yields extra zero-points in $C_V^{(2)}$.

Order $(eV)^3$ component of the nonlinear current is determined by a sum of the two-body contributions W_V and three-body contributions Θ_V. Three-body contributions are described by two independent nonlinear static susceptibilities $\chi^{[3]}_{\uparrow\uparrow\uparrow}$ and $\chi^{[3]}_{\uparrow\downarrow\downarrow}$. Although these nonlinear susceptibilities almost vanish in the Kondo regime, they contribute to the transport outside of the Kondo regime, i.e. in the valence fluctuation, empty orbital, and fully-occupied orbital regimes. The formula shown in Table I reveals the fact that tunnel asymmetries affect $C_V^{(3)}$ only through the cross term $\alpha_{\rm dif}(\Gamma_L-\Gamma_R)/\Delta$, whereas bias asymmetries $\alpha_{\rm dif}$ enter also through the other terms. Thus, the order $(eV)^3$ nonlinear current is not affected by tunnel asymmetries when the bias voltage is applied symmetrically, i.e. $\mu_L=-\mu_R=eV/2$. Conversely, under asymmetrical bias voltages, the coefficient $C_V^{(3)}$ depends on both $\alpha_{\rm dif}$ and $(\Gamma_L-\Gamma_R)/\Delta$. We find that $C_V^{(3)}$ shows a shoulder structure in the valence fluctuation regime in the case where the cross term $\alpha_{\rm dif}(\Gamma_L-\Gamma_R)/\Delta$ are positive and large. It is caused by the peaks that emerge at $\epsilon_d\simeq -U$ and $\epsilon_d\simeq 0$ in the three-body contributions Θ_V. Specifically, these peaks come from one of the two three-body components $\Theta_{\rm II}$ which is enhanced significantly by tunnel and bias asymmetries in this case.

Recently, the three-body contributions Θ_V on the order $(eV)^3$ nonlinear current has been extracted experimentally for quantum dots in a magnetic field [62]. To our knowledge, it is the first observation of three-body effects in the Fermi liquid of the Kondo systems. Our results show that the contributions of $\Theta_{\rm II}$ can be enhanced selectively by tuning tunnel asymmetries keeping the other contributions from $\Theta_{\rm I}$ unchanged, and it leads a characteristic shoulder structure in the gate-voltage dependence of $C_V^{(3)}$. Therefore, it can be used for future analysis to deduce separately the two different components of the three-body correlations, $\chi^{[3]}_{\sigma\sigma\sigma}$ and $\chi^{[3]}_{\sigma\sigma'\sigma'}$ for $\sigma\neq\sigma'$ from measurements. Furthermore, for a multilevel quantum dot such as the SU(N) dot with internal degrees of freedom $\sigma=1,2,\ldots,N$, there is another independent three-body component $\chi^{[3]}_{\sigma\sigma'\sigma''}$ for three different flavors, i.e. σ's [51]. It will give interesting varieties to nonlinear conductance through junctions with tunnel and bias asymmetries, and studies along this line are also in progress.

VIII. ACKNOWLEDGEMENTS

This work was supported by JSPS KAKENHI Grant Nos. JP18K03495, JP18J10205, JP21K03415, JP26220711, and JST CREST Grant No. JPMJCR1876, and the Sasakawa Scientific Research Grant from The Japan Science Society No. 2021-2009.

Appendix A: Low-energy asymptotic form of spectral function

We show here the low-energy asymptotic form of the spectral function $A(\omega,\,T,\,eV)$ in the presence of the tunnel and bias asymmetries which are parametrized by $(\Gamma_L-\Gamma_R)/(\Gamma_L+\Gamma_R)$ and $\alpha_{\rm dif}=\alpha_L-\alpha_R$, respectively.

In order to deduce the coefficients $C_V^{(2)}$ and $C_V^{(3)}$ given in Eqs. (29) and (30) from the Landauer-type formula Eq. (20), we have expanded $A(\omega,\,T,\,eV)$ up to terms of order ω^2, T^2, and $(eV)^2$. Substituting the low-energy asymptotic form of self-energy given in Eqs. (21) and (22) into the retarded Green's function in Eq. (5), we obtain the asymptotic form the spectral function, which is exact up to terms of order ω^2, T^2, and $(eV)^2$:

$$\begin{aligned}\pi\Delta A(\omega,\,T,\,eV)\simeq{}&\sin^2\delta+\pi\sin 2\delta\left[\chi_{\uparrow\uparrow}\,\omega+\frac{1}{2}\left(\alpha_{\rm dif}+\frac{\Gamma_L-\Gamma_R}{\Gamma_L+\Gamma_R}\right)\chi_{\uparrow\downarrow}\;eV\right]\\&+\pi^2\left[\cos 2\delta\left(\chi_{\uparrow\uparrow}^2+\frac{1}{2}\chi_{\uparrow\downarrow}^2\right)-\frac{\sin 2\delta}{2\pi}\chi^{[3]}_{\uparrow\uparrow\uparrow}\right]\omega^2\\&+\pi^2\left[\cos 2\delta\left(\chi_{\uparrow\uparrow}\chi_{\uparrow\downarrow}-\frac{1}{2}\chi_{\uparrow\downarrow}^2\right)-\frac{\sin 2\delta}{2\pi}\chi^{[3]}_{\uparrow\downarrow\downarrow}\right]\left(\alpha_{\rm dif}+\frac{\Gamma_L-\Gamma_R}{\Gamma_L+\Gamma_R}\right)\omega\,eV\\&+\frac{\pi^2}{3}\left(\frac{3}{2}\cos 2\delta\chi_{\uparrow\downarrow}^2-\frac{\sin 2\delta}{2\pi}\chi^{[3]}_{\uparrow\downarrow\downarrow}\right)\left[\left(1+2\alpha_{\rm dif}\frac{\Gamma_L-\Gamma_R}{\Gamma_L+\Gamma_R}+\alpha_{\rm dif}^2\right)\frac{3}{4}(eV)^2+(\pi T)^2\right]+\cdots.\end{aligned}\tag{A1}$$

Appendix B: Fermi-liquid parameters for $|\epsilon_d|\to\infty$

In the limit of $|\epsilon_d|\to\infty$, the Fermi-liquid parameters converge to the values for the noninteracting case $U=0$ [55], in which the phase shift δ^0 and the diagonal element of the linear susceptibility $\chi^{(0)}_{\uparrow\uparrow}$ and that of the three-body

correlations $\chi^{[3](0)}_{\uparrow\uparrow\uparrow}$ are given by

$$\sin 2\delta^{(0)} = \frac{2\Delta\epsilon_d}{\epsilon_d^2+\Delta^2} \xrightarrow{|\epsilon_d|\to\infty} \frac{2\Delta}{\epsilon_d}, \tag{B1}$$

$$\chi^{(0)}_{\uparrow\uparrow} = \frac{1}{\pi}\frac{\Delta}{\epsilon_d^2+\Delta^2} \xrightarrow{|\epsilon_d|\to\infty} \frac{\Delta}{\pi\epsilon_d^2}, \tag{B2}$$

$$\chi^{[3](0)}_{\uparrow\uparrow\uparrow} = \frac{-1}{\pi}\frac{2\Delta\epsilon_d}{(\epsilon_d^2+\Delta^2)^2} \xrightarrow{|\epsilon_d|\to\infty} \frac{-2\Delta}{\pi\epsilon_d^3}. \tag{B3}$$

Furthermore, $\chi^{(0)}_{\uparrow\downarrow}=0$ and $\chi^{[3](0)}_{\uparrow\downarrow\downarrow}=0$ for $U=0$, i.e., the off-diagonal elements of linear and nonlinear susceptibilities for noninteracting electrons vanish and $R-1\to 0$.

Therefore, in the limit of $|\epsilon_d|\to\infty$, the three-body correlations tend to $\Theta_{\rm I}\to -2$ and $\Theta_{\rm II}\to 0$, and thus two-body and three-body parts of $C_V^{(3)}$ approach the following form,

$$W_V \xrightarrow{|\epsilon_d|\to\infty} -\Big(1+3\,\alpha_{\rm dif}^2\Big), \tag{B4}$$

$$\Theta_V \xrightarrow{|\epsilon_d|\to\infty} -2\Big(1+3\,\alpha_{\rm dif}^2\Big) \tag{B5}$$

Thus, $C_V^{(3)}$ depends only on the bias asymmetry and does not on the tunnel asymmetry, as discussed in Eq. (49). Furthermore, the nonlinear current of order $(eV)^2$ vanishes in this limit: $C_V^{(2)} \xrightarrow{|\epsilon_d|\to\infty} 0$.

Appendix C: Alternative interpretation for $C_V^{(2)}$

We describe here an alternative interpretation for the two components of $C_V^{(2)}$ defined in Eqs. (37) and (38). In particular, we show that $\overline{C}_V^{(2a)}$ and $\overline{C}_V^{(2b)}$ can also be interpreted as the contributions caused by the shift of the bias window and the shift of the spectral weight, respectively.

For this purpose, we introduce the conductance $g^{(2)}$ that is determined by the spectral function $A^{(1)}$ given in Eq. (41) which is deduced from order ω and eV terms of the self-energy,

$$g^{(2)} \equiv g_0\,\frac{\partial}{\partial eV}\int_{-\alpha_R eV}^{\alpha_L eV} d\omega\,\pi\Delta A^{(1)}(\omega,eV), \tag{C1}$$

where $g_0=(2e^2/h)4\Gamma_L\Gamma_R/(\Gamma_L+\Gamma_R)^2$. This conductance $g^{(2)}$ describes the nonlinear current exactly up to terms of order $(eV)^2$.

We also consider the following contributions, using the spectral function $A^{(1)}(\omega,eV)$ for $\alpha=0$,

$$\begin{aligned} g^{(1)} &\equiv g_0\,\frac{\partial}{\partial eV}\int_{-\frac{1}{2}eV}^{\frac{1}{2}eV} d\omega\;\pi\Delta A^{(1)}(\omega,eV)\Big|_{\alpha=0} \\ &= g_0\,\sin^2\delta + O\big((eV)^2\big). \end{aligned} \tag{C2}$$

The last line shows that this term $g^{(1)}$ describes the linear conductance. We now decompose the conductance $g^{(2)}$ into the following form, by introducing another term $g^{(2)}_{\rm ref}$ as a reference,

$$g^{(2)} = g^{(1)} + \Big[g^{(2)}_{\rm ref}-g^{(1)}\Big] + \Big[g^{(2)}-g^{(2)}_{\rm ref}\Big], \tag{C3}$$

$$g^{(2)}_{\rm ref} = g_0\,\frac{\partial}{\partial eV}\int_{-\alpha_R eV}^{\alpha_L eV} d\omega\;\pi\Delta A^{(1)}(\omega,eV)\Big|_{\alpha=0}. \tag{C4}$$

Here, $g^{(2)}_{\rm ref}-g^{(1)}$ represents variation of the current caused by the shift of the bias window from the symmetric position because the integrand $A^{(1)}(\omega,eV)\big|_{\alpha=0}$ is common for $g^{(2)}_{\rm ref}$ and $g^{(1)}$,

$$g^{(2)}_{\rm ref}-g^{(1)} = g_0\,\frac{\pi\sin 2\delta}{4}\,\alpha_{\rm dif}\left(\frac{eV}{T^*}\right)+\cdots. \tag{C5}$$

This term is identical to the one with the coefficient $\overline{C}_V^{(2a)}$, defined in Eq. (37). The remaining term $g^{(2)}-g^{(2)}_{\rm ref}$ represents variation of the current caused by the shift of the spectral weight as the integrand for this term can be rewritten into the difference $A^{(1)}(\omega,eV)-A^{(1)}(\omega,eV)\big|_{\alpha=0}$,

$$g^{(2)}-g^{(2)}_{\rm ref} = -g_0\,\frac{\pi\sin 2\delta}{4}\,2\alpha\,(R-1)\left(\frac{eV}{T^*}\right)+\cdots. \tag{C6}$$

This term also corresponds to the one described with the coefficient $\overline{C}_V^{(2b)}$.

[1] J. Kondo, Prog. Theor. Phys. **32**, 37 (1964).
[2] A. C. Hewson, *The Kondo Problem to Heavy Fermions* (Cambridge University Press, Cambridge, U.K., 1993).
[3] P. W. Anderson, Phys. Rev. **124**, 41 (1961).
[4] P. Nozières, J. Low Temp. Phys. **17**, 31 (1974).
[5] K. G. Wilson, Rev. Mod. Phys. **47**, 773 (1975).
[6] K. Yamada, Prog. Theor. Phys. **53**, 970 (1975).
[7] K. Yamada, Prog. Theor. Phys. **54**, 316 (1975).
[8] H. Shiba, Prog. Theor. Phys. **54**, 967 (1975).
[9] A. Yoshimori, Prog. Theor. Phys. **55**, 67 (1976).
[10] T. K. Ng and P. A. Lee, Phys. Rev. Lett. **61**, 1768 (1988).
[11] L. I. Glazman and M. E. Raikh, JETP Lett. **47**, 452 (1988).
[12] Y. Meir, N. S. Wingreen, and P. A. Lee, Phys. Rev. Lett.

66, 3048 (1991).
[13] A. Kawabata, J. Phys. Soc. Japan **60**, 3222 (1991).
[14] D. Goldhaber-Gordon, H. Shtrikman, D. Mahalu, D. Abusch-Magder, U. Meirav, and M. A. Kastner, Nature **391**, 156 (1998).
[15] D. Goldhaber-Gordon, J. Göres, M. A. Kastner, H. Shtrikman, D. Mahalu, and U. Meirav, Phys. Rev. Lett. **81**, 5225 (1998).
[16] S. M. Cronenwett, T. H. Oosterkamp, and L. P. Kouwenhoven, Science **281**, 540 (1998).
[17] W. G. van der Wiel, S. D. Franceschi, T. Fujisawa, J. M. Elzerman, S. Tarucha, and L. P. Kouwenhoven, Science **289**, 2105 (2000).
[18] I. V. Borzenets, J. Shim, J. C. H. Chen, A. Ludwig, A. D. Wieck, S. Tarucha, H.-S. Sim, and M. Yamamoto, Nature **579**, 210 (2020).
[19] J. Schmid, J. Weis, K. Eberl, and K. v. Klitzing, Physica B: Condens. Matter **256-258**, 182 (1998).
[20] F. Simmel, R. H. Blick, J. P. Kotthaus, W. Wegscheider, and M. Bichler, Phys. Rev. Lett. **83**, 804 (1999).
[21] S. Sasaki, S. Amaha, N. Asakawa, M. Eto, and S. Tarucha, Phys. Rev. Lett. **93**, 017205 (2004).
[22] M. Grobis, I. G. Rau, R. M. Potok, H. Shtrikman, and D. Goldhaber-Gordon, Phys. Rev. Lett. **100**, 246601 (2008).
[23] G. D. Scott, Z. K. Keane, J. W. Ciszek, J. M. Tour, and D. Natelson, Phys. Rev. B **79**, 165413 (2009).
[24] O. Zarchin, M. Zaffalon, M. Heiblum, D. Mahalu, and V. Umansky, Phys. Rev. B **77**, 241303(R) (2008).
[25] T. Delattre, C. Feuillet-Palma, L. G. Herrmann, P. Morfin, J.-M. Berroir, G. FShu ve, B. PlaXun ais, D. C. Glattli, M.-S. Choi, C. Mora, and T. Kontos, Nat. Phys. **5**, 208 (2009).
[26] Y. Yamauchi, K. Sekiguchi, K. Chida, T. Arakawa, S. Nakamura, K. Kobayashi, T. Ono, T. Fujii, and R. Sakano, Phys. Rev. Lett. **106**, 176601 (2011).
[27] W. Izumida, O. Sakai, and Y. Shimizu, J. Phys. Soc. Japan **67**, 2444 (1998).
[28] A. Oguri, Phys. Rev. B **64**, 153305 (2001).
[29] F. B. Anders, Phys. Rev. Lett. **101**, 066804 (2008).
[30] A. Weichselbaum and J. von Delft, Phys. Rev. Lett. **99**, 076402 (2007).
[31] W. Izumida and O. Sakai, Phys. Rev. B **62**, 10260 (2000).
[32] L. Borda, G. Zaránd, W. Hofstetter, B. I. Halperin, and J. von Delft, Phys. Rev. Lett. **90**, 026602 (2003).
[33] E. A. Laird, F. Kuemmeth, G. A. Steele, K. Grove-Rasmussen, J. Nygård, K. Flensberg, and L. P. Kouwenhoven, Rev. Mod. Phys. **87**, 703 (2015).
[34] Y. Teratani, R. Sakano, R. Fujiwara, T. Hata, T. Arakawa, M. Ferrier, K. Kobayashi, and A. Oguri, J. Phys. Soc. Japan **85**, 094718 (2016).
[35] M. Ferrier, T. Arakawa, T. Hata, R. Fujiwara, R. Delagrange, R. Weil, R. Deblock, R. Sakano, A. Oguri, and K. Kobayashi, Nat. Phys. **12**, 230 (2016).
[36] M. Ferrier, T. Arakawa, T. Hata, R. Fujiwara, R. Delagrange, R. Deblock, Y. Teratani, R. Sakano, A. Oguri, and K. Kobayashi, Phys. Rev. Lett. **118**, 196803 (2017).
[37] Y. Teratani, R. Sakano, T. Hata, T. Arakawa, M. Ferrier, K. Kobayashi, and A. Oguri, Phys. Rev. B **102**, 165106 (2020).
[38] S. Sasaki, S. De Franceschi, J. M. Elzerman, W. G. van der Wiel, M. Eto, S. Tarucha, and L. P. Kouwenhoven, Nature **405**, 764 (2000).
[39] P. Jarillo-Herrero, J. Kong, H. S. van der Zant, C. Dekker, L. P. Kouwenhoven, and S. De Franceschi, Nature **434**, 484 (2005).
[40] M.-S. Choi, R. López, and R. Aguado, Phys. Rev. Lett. **95**, 067204 (2005).
[41] M. Eto, J. Phys. Soc. Japan **74**, 95 (2005).
[42] R. Sakano and N. Kawakami, Phys. Rev. B **73**, 155332 (2006).
[43] R. Sakano, T. Kita, and N. Kawakami, J. Phys. Soc. Japan **76**, 074709 (2007).
[44] A. Makarovski, A. Zhukov, J. Liu, and G. Finkelstein, Phys. Rev. B **75**, 241407(R) (2007).
[45] F. B. Anders, D. E. Logan, M. R. Galpin, and G. Finkelstein, Phys. Rev. Lett. **100**, 086809 (2008).
[46] I. Weymann, R. Chirla, P. Trocha, and C. P. Moca, Phys. Rev. B **97**, 085404 (2018).
[47] C. Mora, P. Vitushinsky, X. Leyronas, A. A. Clerk, and K. Le Hur, Phys. Rev. B **80**, 155322 (2009).
[48] C. Mora, Phys. Rev. B **80**, 125304 (2009).
[49] J. P. Cleuziou, N. V. N'Guyen, S. Florens, and W. Wernsdorfer, Phys. Rev. Lett. **111**, 136803 (2013).
[50] D. Mantelli, C. P. Moca, G. Zaránd, and M. Grifoni, Physica E **77**, 180 (2016).
[51] Y. Teratani, R. Sakano, and A. Oguri, Phys. Rev. Lett. **125**, 216801 (2020).
[52] E. Sela and J. Malecki, Phys. Rev. B **80**, 233103 (2009).
[53] A. A. Aligia, J. Phys.: Condens. Matter **24**, 015306 (2011).
[54] A. C. Hewson, J. Phys.: Condens. Matter **13**, 10011 (2001).
[55] C. Mora, C. P. Moca, J. von Delft, and G. Zaránd, Phys. Rev. B **92**, 075120 (2015).
[56] M. Filippone, C. P. Moca, A. Weichselbaum, J. von Delft, and C. Mora, Phys. Rev. B **98**, 075404 (2018).
[57] A. Oguri and A. C. Hewson, Phys. Rev. Lett. **120**, 126802 (2018).
[58] A. Oguri and A. C. Hewson, Phys. Rev. B **97**, 045406 (2018).
[59] A. Oguri and A. C. Hewson, Phys. Rev. B **97**, 035435 (2018).
[60] H. R. Krishna-murthy, J. W. Wilkins, and K. G. Wilson, Phys. Rev. B **21**, 1003 (1980).
[61] K. Tsutsumi, Y. Teratani, A. Oguri, and R. Sakano, JPS Conf. Proc **30**, 011174 (2020).
[62] T. Hata, Y. Teratani, T. Arakawa, S. Lee, M. Ferrier, R. Deblock, R. Sakano, A. Oguri, and K. Kobayashi, Nature Communications **12**, 3233 (2021).
[63] Y. Meir and N. S. Wingreen, Phys. Rev. Lett. **68**, 2512 (1992).
[64] S. Hershfield, J. H. Davies, and J. W. Wilkins, Phys. Rev. B **46**, 7046 (1992).
[65] A. C. Hewson, A. Oguri, and D. Meyer, Eur. Phys. J. B **40**, 177 (2004).
[66] P. Dutt, J. Koch, J. Han, and K. Le Hur, Annals of Physics **326**, 2963 (2011) .
[67] G. Zaránd, L. Borda, J. von Delft, and N. Andrei, Phys. Rev. Lett. **93**, 107204 (2004) .
[68] S. Kehrein, Phys. Rev. Lett. **95**, 056602 (2005).